Brain Research 1799 (2023) 148180

Contents lists available at ScienceDirect

Brain Research

journal homepage: www.elsevier.com/locate/brainres

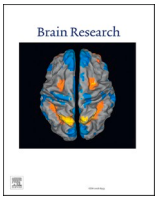

Impact of neuroinflammation on epigenetic transcriptional control of Sonic Hedgehog members in the central nervous system

Mariana Ribeiro Costa [a,1], Amanda Yasmin Ilario dos Santos [a,1], Taís Browne de Miranda [a], Rogério Aires [b], Alex de Camargo Coque [b], Elizabeth Cristina Perez Hurtado [b], Maria Martha Bernardi [b], Vanessa Gallego Arias Pecorari [f], Denise Carleto Andia [f], Alexander Birbrair [e], Gilles J. Guillemin [d], Alexandra Latini [c], Rodrigo A. da Silva [a,b,*]

[a] School of Dentistry, University of Taubaté, 12020-3400 Taubaté, São Paulo, Brazil
[b] Epigenetic Study Center and Gene Regulation – CEEpiRG, Program in Environmental and Experimental Pathology, Paulista University, São Paulo 04026-002, São Paulo, Brazil
[c] Bioenergetics and Oxidative Stress Lab – LABOX, Department of Biochemistry, Center for Biological Sciences, Federal University of Santa Catarina, Florianopolis, Brazil
[d] Neuroinflammation Group, Faculty of Medicine, Health and Human Sciences, Macquarie University, Sydney, NSW 2109, Australia
[e] Department of Pathology, Federal University of Minas Gerais, Belo Horizonte, MG, Brazil
[f] School of Dentistry, Health Science Institute, Paulista University, São Paulo 04026-002, São Paulo, Brazil

ARTICLE INFO

Keywords:
Neuroepigenetics
Sonic Hedgehog
Neuroinflammation
DNA methylation
SUFU hypermethylation
DNA-modifying

ABSTRACT

Sonic Hedgehog (Shh) signaling plays a critical role during central nervous system (CNS) development, and its dysregulation leads to neurological disorders. Nevertheless, little is known about Shh signaling regulation in the adult brain. Here, we investigated the contribution of DNA methylation on the transcriptional control of Shh signaling pathway members and its basal distribution impact on the brain, as well as its modulation by inflammation. The methylation status of the promoter regions of these members and the transcriptional profile of DNA-modifying enzymes (DNA Methyltransferases – DNMTs and Tet Methylcytosine Dioxygenase – TETs) were investigated in a murine model of neuroinflammation by qPCR. We showed that, in the adult brain, methylation in the CpG promoter regions of the Shh signaling pathway members was critical to determine the endogenous differential transcriptional pattern observed between distinct brain regions. We also found that neuroinflammation differentially modulates gene expression of DNA-modifying enzymes. This study reveals the basal transcriptional profile of DNMTs and TETs enzymes in the CNS and demonstrates the effect of neuroinflammation on the transcriptional control of members of the Shh Signaling pathway in the adult brain.

1. Introduction

The hedgehog signaling has been defined as a morphogenic pathway that regulates embryo development and adult tissue maintenance. Sonic hedgehog (SHH) is one of the most widespread ligands of the hedgehog pathway and a long-range morphogen that controls neural tube formation, limbs axial skeleton during early embryogenesis (Antonelli at al., 2019) and tissue homeostasis, especially in the central nervous system (CNS) (Varjosalo and Taipale, 2008). Ligands of the hedgehog pathway act as mitogens regulating, in an autocrine and paracrine manner, cell proliferation and differentiation during organogenesis (Ingham and McMahon, 2001), acquisition of polarity and the control of left-right asymmetry during member development (Hammerschmidt et al., 1997). Once released, SHH binds the inhibitory receptor patched 1 (PTCH1), leading to the activation of the cell-surface receptor Smoothened (Smo) and subsequently drives the transcription of glioma-associated oncogene homolog (GLI1) target genes in mammals (Tukachinsky et al., 2010).

SHH signaling is fundamental for the maintenance of neuronal activity, and impairment of SHH-driven cascade is associated with

* Corresponding author at: Programa de Pós-Graduação em Ciências da Saúde, Universidade de Taubaté – UNITAU / Programa de Pós-Graduação em Patologia Ambiental e Experimental, Universidade Paulista – UNIP, Brazil.
E-mail addresses: elizabeth.hurtado@docente.unip.br (E.C.P. Hurtado), vanessa.pecorari@docente.unip.br (V.G.A. Pecorari), denise.andia@docente.unip.br (D.C. Andia), gilles.guillemin@mq.edu.au (G.J. Guillemin), rodrigo.silva3@docente.unip.br (R.A. da Silva).
[1] Contributed equally in this study.

https://doi.org/10.1016/j.brainres.2022.148180
Received 3 August 2022; Received in revised form 14 September 2022; Accepted 23 November 2022
Available online 1 December 2022

Fig. 1. Schematic representation of the amplified region of the Hedgehog pathway members. The amplified sequence shows the location of the gene on the chromosome and the location of the fragment of the studied promoter region of the gene. The primer is represented in red and the cutting site of the *Msp*I and *Hpa*II endonucleases in yellow.

senescence and greater susceptibility to develop disorders frequently linked to the aging process (Dashti et al., 2012; Han et al., 2008). There is a body of evidence showing that the mitogenic activity of the SHH pathway not only signals during development but also can be reactivated during adulthood, mainly to repair tissues (Bambakidis et al., 2012). Indeed, it has been shown that the hedgehog signaling is not activated in the healthy brain; however, it is increased after brain injury, promoting tissue repairing. In this scenario, it has been shown that SHH regulates the ability of mature astrocytes to behave as neural progenitors after ischemia and acute cerebral CTX lesions (Sirko et al., 2013; Sims et al., 2009; Pitter et al., 2014; Amankulor et al., 2009). It has also been shown that SHH positively upregulates the expression of anti-apoptotic genes and inhibits the expression of the BCL2 Associated X, Apoptosis Regulator (Bax), a pro-apoptotic gene, in cortical neurons exposed to H_2O_2 (Dai et al., 2011), and attenuates the immune response by decreasing the expression of pro-inflammatory mediators and leukocyte adhesion/migration in blood–brain barrier's endothelial cells (Alvarez-Buylla and Ihrie, 2014). These examples remark the crucial role of SHH as an antioxidant and anti-inflammatory mediator, contributing to the maintenance of neurogenesis and repairing of the CNS, being therefore, a potential target for therapeutic interventions in CNS disorders (Chen et al., 2018).

In recent years, an increasing amount of evidence has shown the role of DNA methylation in the development and progression of many complex diseases, mainly linked to aging, such as cancer, cardiovascular diseases and neurodegenerative disorders that at the molecular level, cause changes in the gene expression, underlying the decline in physiological function (Pagiatakis et al., 2021). It has been demonstrated that the regulatory promoter region of the activating protein of SHH and the other members of the hedgehog pathway, including GLI1, fusion suppressor (SUFU) and the transmembrane receptor PTCHD1 have numerous CpG islands, which are subject to methylation, and therefore to epigenetic transcriptional regulation (Wils and Bijlsma, 2018). Compromised expression of SHH, PTCHD1 and human hedgehog interacting protein (HHIP) genes due to hypermethylation of their promoter regions have been shown to be involved in the development of medulloblastoma, a type of neuroectodermal tumor (Shahi et al., 2015; Shahi et al., 2010). Furthermore, the development of rheumatoid arthritis, a chronic autoimmune inflammatory disease, has been shown to be linked to hypermethylation of the PTCHD1 promoter and reduction of its gene expression and protein content, resulting in increased secretion of pro-inflammatory cytokines, Interleukin 6 (IL 6) and Tumor Necrosis Factor- α (TNF-α) (Sun et al., 2017).

Based on the information about the involvement of SHH in inflammatory pathological conditions and CNS defense mechanisms and the differential transcriptional profile of limbs in different brain regions, we posit that DNA methylation may be the driving force responsible by the differential basal transcriptional profile of the hedgehog members signaling pathway and hypothesizing a direct effect of neuroinflammation on the epigenetic control of the signaling pathway of hedgehog members. In order to prove this, we treated male adult mice with a single lipopolysaccharide (LPS) dose (0.33 mg/kg) and DNA methylation, as well as the transcription profile of the hedgehog pathway members were assessed (See Fig. 1).

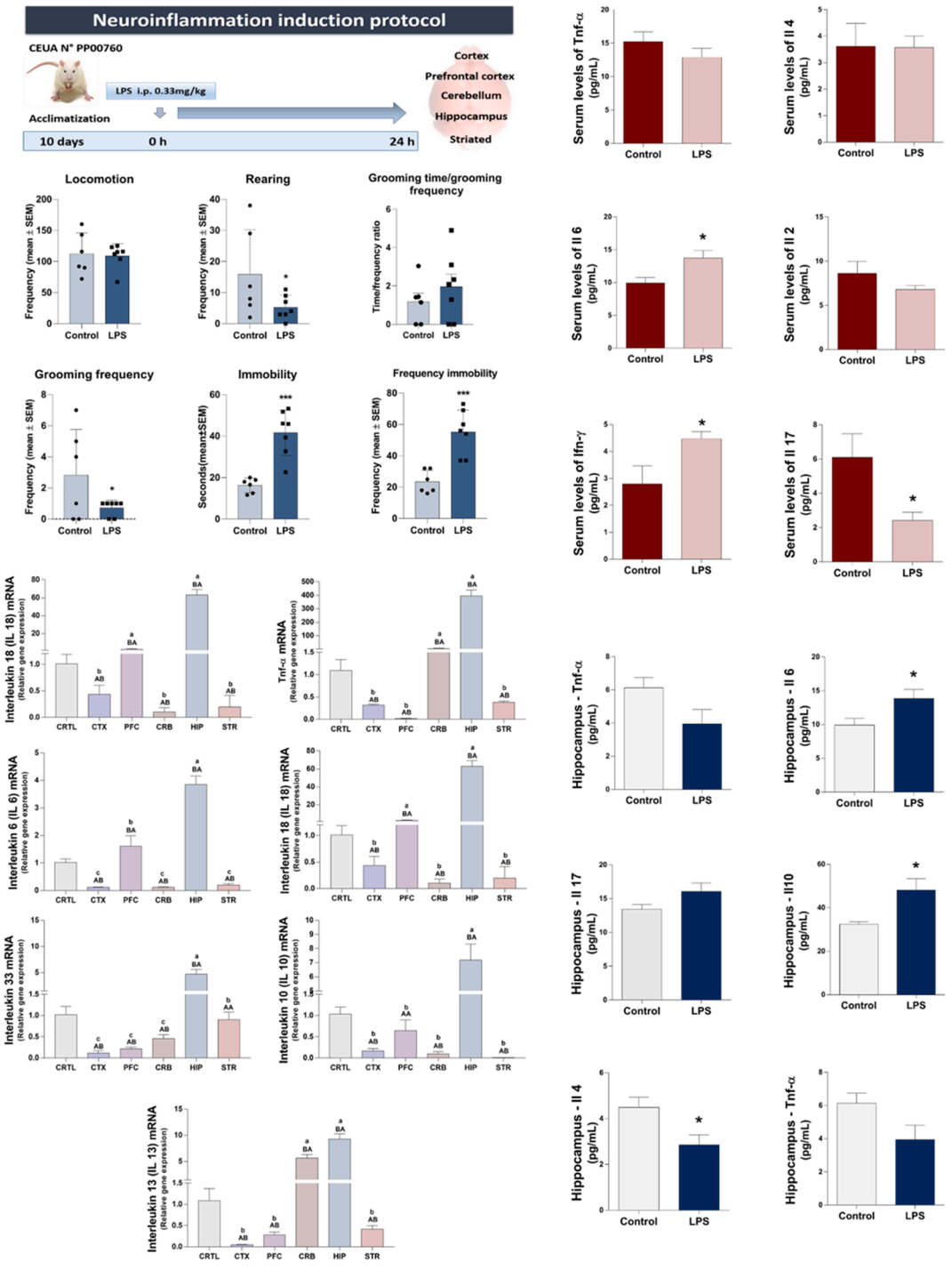

Fig. 2. Gene expression analysis of Inflammatory Cytokines in the Central Nervous System: (a) Graphical representation of the experimental model. (b-g) Behavioral analysis. (h-m) Serum concentration of cytokines and (u-z) Concentration of cytokines in the Hippocampus (HIP). After RNA extraction using the TRIzol® method, the transcriptional profile of the proinflammatory cytokines *Il 1β* (n), *Tnf-α* (o), *Il 6* (p), *Il 18* (q), *Il 33* (r) and antiinflammatory cytokines *Il 10* (s) and *Il 13* (t) were evaluated by reactions of qPCR in the different brain structures after 24 h of LPS administration (0.33 mg/Kg). The *Gapdh*, *β-actin* and *18 s* genes were used as normalizers. The results were calculated using the method ($2^{-\Delta Ct}$) and represent the mean ± standard deviation of 5 independent animals performed in technical duplicate. Different letters indicate a statistically significant difference. Capital letters compare groups with and without LPS within each analyzed region and lowercase letters compare the expression of each cytokine within each brain region.

2. Results

2.1. Neuroinflammatory effect characterization of intraperitoneal LPS administration

To confirm the sick-like behavior, we first investigated the effect of LPS (0.33 mg/kg; single injection) on animal behavior, as demonstrated by the experimental scheme shown in Fig. 2a. The results presented in Fig. 2b-**g** demonstrated the rearing ($t = 1.71$, $df = 19$, $p < 0.05$) (Fig. 2c) and grooming frequencies ($t = 2.61$, $df = 19$, $p = 0.009$) (Fig. 2e) were decreased in LPS group relative to controls. Additionally, the time ($t = 5.40$, $df = 11$, $p = 0.0002$) and frequency ($t = 4.94$, $df = 11$, $p = 0.0004$)

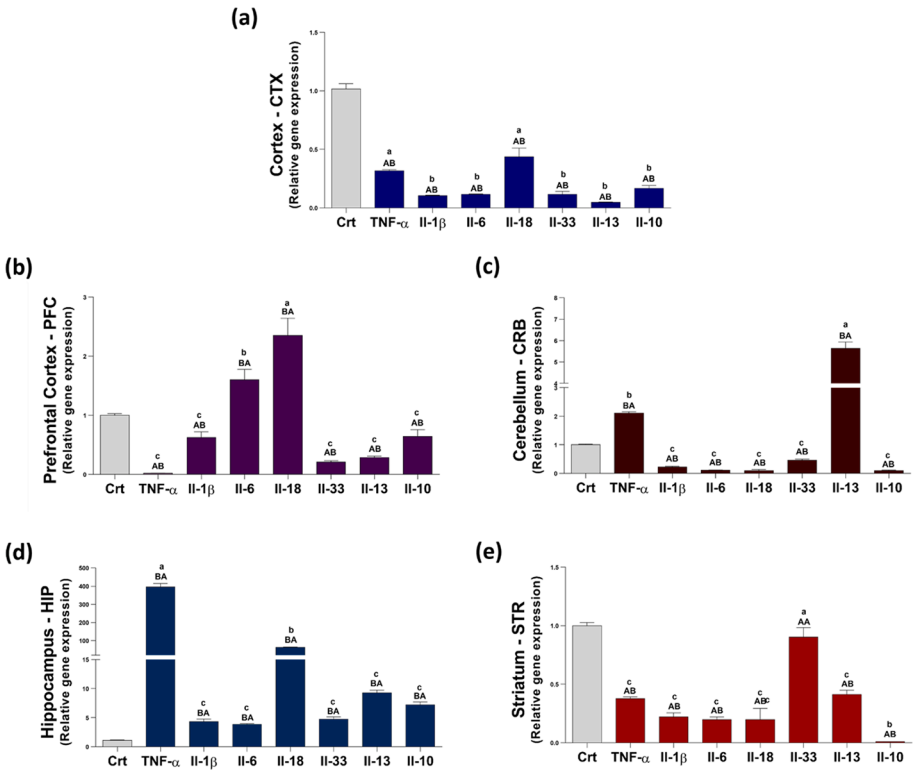

Fig. 3. Graphic representation of the relative expression of different cytokines in different brain regions. Graphic representation of the relative gene expression of different inflammatory cytokines in Cortex (CTX) (a), Prefrontal Cortex (PFC) (b), Cerebellum (CRB) (c), Hippocampus (HIP) (d) and Striatum (STR) (e) determined by qPCR. The results represent the mean ± standard deviation of 5 independent animals performed in technical duplicate. Different letters indicate a statistically significant difference. Capital letters compare groups with and without LPS within each analyzed region and lowercase letters compare the expression of each cytokine within each brain region.

of immobility were increased in the LPS group relative to control group (Fig. 2f,**g**). No significant differences were observed for locomotion (Fig. 2b) and grooming time (Fig. 2d). Then, the concentration of serum cytokines was determined, and a significant increase in the circulating concentration of Il 6 (Fig. 2j) and Interferon Gamma (Ifn-γ) (Fig. 2l), with a decrease in the concentration of Interleukin 17 (Il 17) (Fig. 2m)

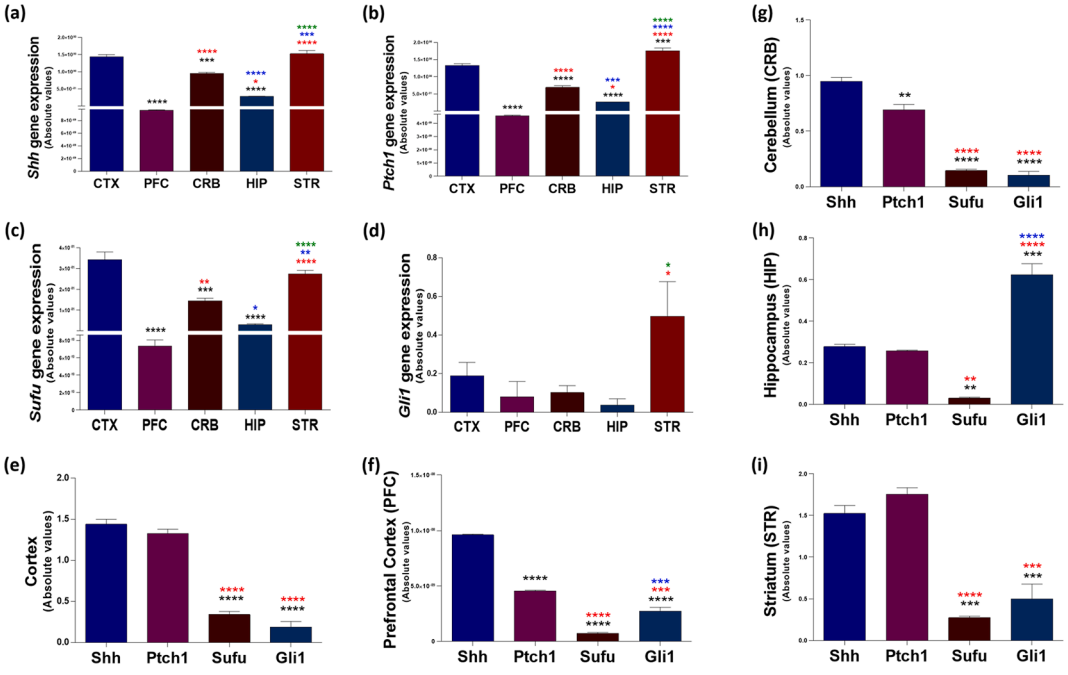

Fig. 4. Transcriptional profile of members of the Hedgehog members in the Central Nervous System. The transcriptional profile of members of the Hedgehog members was determined after RNA extraction using the TRIzol® method, the transcriptional profile of the Sonic Hedgehog – *Shh* (a), Patched 1 – *Ptchd1* (b), Oncogene Homolog fusion suppressor - *Sufu* (c), Glioma-Associated 1 – *Gli1* (d) were evaluated by reactions of qPCR in the different brain structures after 24 h of LPS administration (0.33 mg/kg). Graphical representation of the absolute values of gene expression of Via Hedgehog members in the different brain structures (e-i). The *Gapdh*, *β-actin* and *18 s* genes were used as normalizers. The results were calculated using the method ($2^{-\Delta Ct}$) and represent the mean ± standard deviation of 5 independent animals performed in technical duplicate. The results represent the mean ± standard deviation of 5 independent animals performed in technical duplicate. Different letters indicate a statistically significant difference. Capital letters compare groups with and without LPS within each analyzed region and lowercase letters compare the expression of each cytokine within each brain region.

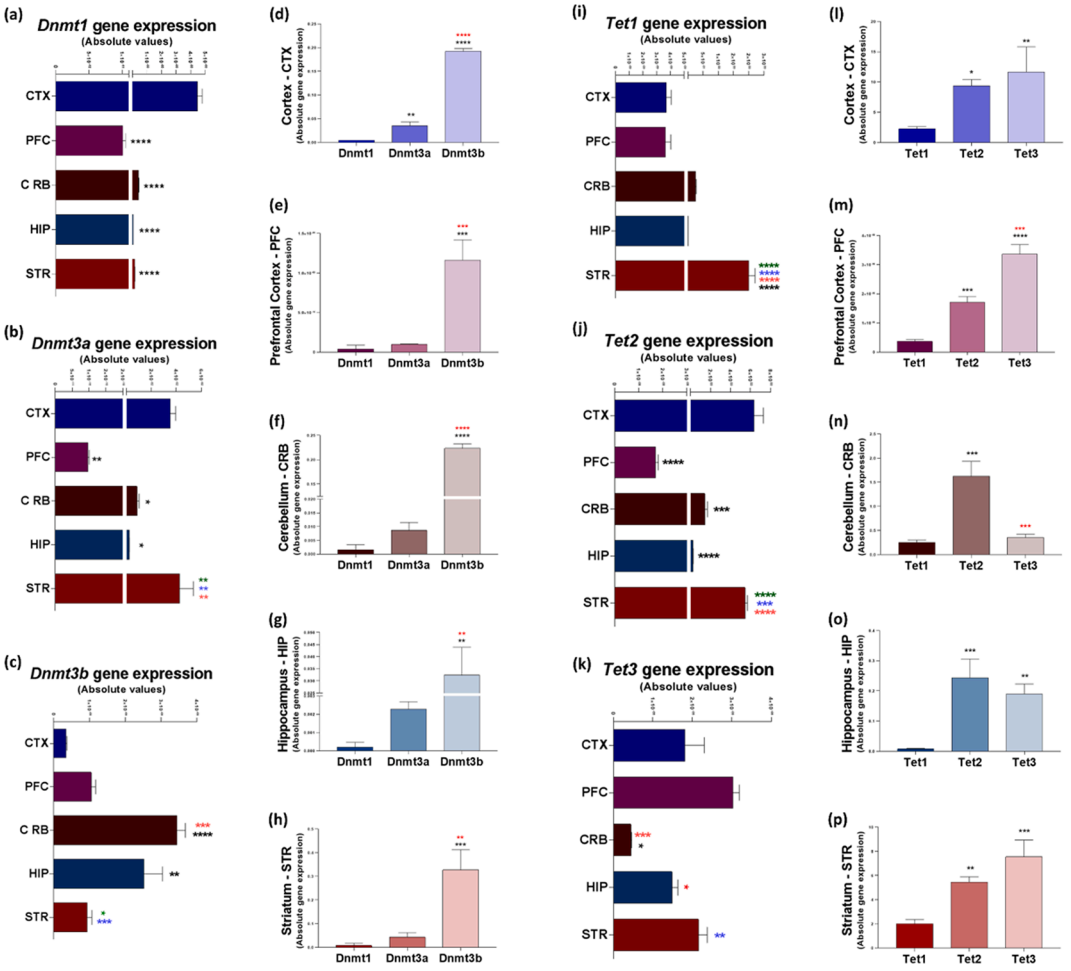

Fig. 5. Transcriptional profile of DNA methylation modifying enzymes in the Central Nervous System. The transcriptional profile of DNA methyltransferases [*Dnmt1* (a); *Dmnt3a* (b); *Dnmt3b* (c)] and DNA demethylases [*Tet1* (i); *Tet2* (j); *Tet3* (k)] was by qPCR determined after RNA extraction using the TRIzol® method of different brain structures. Graphical representation of the absolute values of gene expression of DNA methyltransferases (d, e, f, g, h) and DNA demethylases (l, m. n. o. p) in the different brain structures. The *Gapdh*, *β-actin* and *18 s* genes were used as normalizers. The results were calculated using the method ($2^{-\Delta Ct}$) and represent the mean ± standard deviation of 5 independent animals performed in technical duplicate. The lowercase letters compare the expression of each cytokine within each brain region. Significant statistical differences when compared to the Cortex (CTX) group or Dnmt1 or Tet1 expression * $p < 0.05$; ** $p < 0.001$ and *** $p < 0.0001$, * $p < 0.05$; ** $p < 0.001$ and *** $p < 0.0001$ when compared to the PFC (PFC) group or Dnmt3a or Tet2 expression; * $p < 0.05$; ** $p < 0.001$ and *** $p < 0.0001$ when compared to the Cerebellum (CRB); * $p < 0.05$; ** $p < 0.001$ and *** $p < 0.0001$ when compared to Hippocampus (HIP) group.

were observed. After confirmation of disease-like behavior and activation of the immune response, the brain structures were dissected out for RNA isolation, after 24 h of the LPS injection. The differential transcriptional profile was observed between the brain structures of treated animals with LPS, as compared to saline-treated animals (CTRL), for both anti and proinflammatory cytokines (Fig. 2n-**t**). The Hippocampus (HIP) was the only structure that showed high levels of proinflammatory cytokines gene expression, with statistically significant difference [Interleukin 1β (*Il 1β*) - Fig. 2n; *Il 6* - Fig. 2p; Interleukin 33 (*Il 33*) - Fig. 2r and *Tnf*- α - Fig. 2o), in contrast with the Prefrontal Cortex (PFC) and Cerebellum (CRB) that showed an increase in the *Il 6* gene expression (Fig. 2p) and *Tnf*-α (Fig. 2o)], respectively. We also observed a significant increase in the expression of the anti-inflammatory cytokines Interleukin 18 (*Il 18*) and Interleukin 13 (*Il 13*) in the HIP (Fig. 2q, **t**), *Il 18* in the PFC (Fig. 2q) and in the CRB for *Il 13* (Fig. 2t). For the other structures, the expression of anti-inflammatory cytokines was reduced (Fig. 2q, **t**). Since the HIP was the most sensitive region to neuroinflammation, the concentration of cytokines was determined. Amongst the evaluated cytokines, *Il 6* and Interleukin 10 (*Il 10*) showed an increase in the concentration (Fig. 2v, **x**) while a decrease in the Interleukin 4 (*Il 4*) was observed (Fig. 2y), in the LPS group.

After determining the transcriptional pattern of cytokines, their individual profile was represented after the LPS administration, in each one of the brain regions. The results presented in Fig. 3 show all cytokines were decreased in the Cortex (CTX) (Fig. 3a) while there was an increase in the HIP (Fig. 3d), with *Tnf- α* and *Il 18* (Fig. 3d) being the most significant. In the PFC, we observed a predominant expression of the proinflammatory cytokines *Il 6* and *Il 18* (Fig. 3b), while in the CRB, there was a decrease in all cytokines, except for *Tnf-α* and *Il 13* (Fig. 3c). Similarly, to the CTX, all cytokines were also decreased in the Striatum (STR), except for *Il 33,* with minimum detectable amount of the *Il 10* (Fig. 3e). All the above results can be observed with statistical details in the **Table S1**. The results of all cytokines presented so far demonstrated there were differences for groups (CTRL × LPS) and brain regions, with significant interaction (**Table S1**).

2.2. *DNA methylation contributes to the differential expression of Hedgehog pathway members in the CNS*

To investigate the involvement of DNA methylation in the transcriptional control of Hedgehog pathway members, the transcriptional profile was initially determined in different areas of the brain. The results presented in Fig. 4 show different values in the amount of transcripts between the brain structures (Fig. 4a-d), highlighting the PFC as

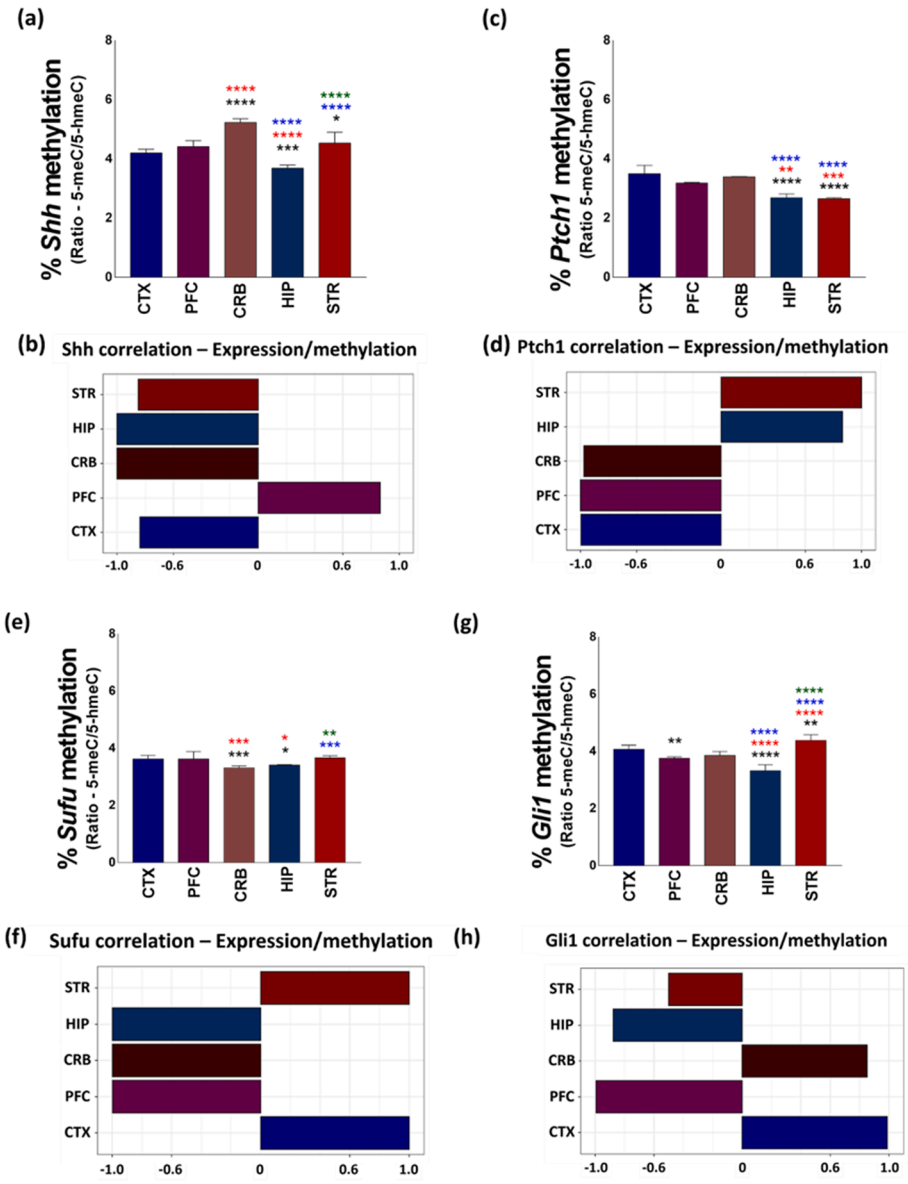

Fig. 6. Epigenetic landscape of Hedgehog members on Central Nervous System. The gene promoter hydroxymethylation/methylation patterns were investigated by DNA glucosylation by T4-BGT and *Msp*I and *Hpa*II digestion followed by qPCR analysis with specific primers. The DNA methylation status of the Hedgehog members [Sonic Hedgehog – *Shh* gene (a), Patched 1 – *Ptchd1* gene (c), Oncogene Homolog fusion suppressor - *Sufu* gene (e) and Glioma-Associated 1 – *Gli1* gene (g). Relation between gene promotor methylation status and expression of Shh (b), Ptch1 (d), Sufu (f) and Gli1 (h). Graphic representation of the basal epigenetic panoram of the members of the Hedgehog pathway in different brain structures (i-m). The relative methylation levels were presented as a 5-meC/5-hmeC ratio and determined using the cycle threshold (Ct) method and the methylation results are presented as Ct [*Hpa*II] – Ct [*Msp*I] /Ct [SE] and the hydroxymethylation results are presented as Ct [*Msp*I] Ct [SE]. Results were represented as mean ± standard deviation of 5 independent animals performed in technical duplicate. The lowercase letters compare the expression of each cytokine within each brain region and symbols (+, *, #) compare Shh member types within the same brain region.

the region presenting the lowest levels of all Hedgehog pathway members; in addition, a differential transcriptional profile was observed between the members of the pathway in the same structure (Fig. 4e**-i**). Most of the brain structures presented high levels of the ligand *Shh* and its receptor *Ptchd1*, compared to *Sufu* and *Gli1* basal levels **(**Fig. 4e**, g, h)**, except for the PFC, in which statistical differences were not demonstrated among the members of the pathway analyzed (Fig. 4f**).** All the above results can also be observed with statistical details in the **Table S2**.

Based on the results of the characterization of the differential transcriptional profile of the Hedgehog pathway components in the CNS, the next stage was to determine the transcriptional profile of the DNA methylation-modifying enzymes, DNMTs and TETs, and the methylation status of the promoter region of the Hedgehog members. The results presented in Fig. 5, indicate DNA methyltransferase 1 (*Dnmt1*) was the most expressed *Dnmt* in the CTX, while DNA methyltransferase 3a (*Dnmt3a*) and DNA methyltransferase 3b (*Dnmt3b*) were the most expressed in the STR (Fig. 5a-c**).** The CTX was the brain structure that showed the highest levels of all *Tets*. In detail, the PFC was the brain structure that presented the lowest levels of all *Dnmts* (Fig. 5a-c) and *Tets* (Fig. 5i**-k).** Conversely, when the basal levels of the DNA methylation-modifying enzymes were compared in each one of the brain structures, the *Dnmt3b* presented the most increased levels among all *Dnmts*, while Tet methylcytosine dioxygenase 1 (*Tet1*) presented the most decreased levels. Curiously, although the CRB presented low levels of Tet methylcytosine dioxygenase 2 (T*et2*) compared to the other brain regions, the expression of this enzyme was the highest among all *Tets* in this brain region.

The results shown in Fig. S1a-e demonstrated there is a tendency of DNA hydroxymethylation in all brain regions analyzed, with statistical differences for CTX and STR (Fig. S1a, e**).** All the above results can also be observed with statistical details in the **Table S3**. Next, we decided to assess whether the absolute expression of *Shh*, *Ptchd1*, *Sufu* and *Gli1* genes could be epigenetically controlled. For this, we determined the methylation status of their promoter region and compared to the absolute expression values, using the Pearson's correlation test. In general, the results (Fig. 6) point to the HIP being the less methylated brain structure, for all Hedgehog pathway members. In addition, most of the brain regions presented an inverse correlation, with the r values almost reaching 1 for all Hedgehog pathway members, being observed a direct proportional correlation for Shh (PFC), Sufu (STR, CTX), Ptchd1 (STR, HIP) and Gli1 (CRB, CTX) (Fig. 6b, f, d**, h**).

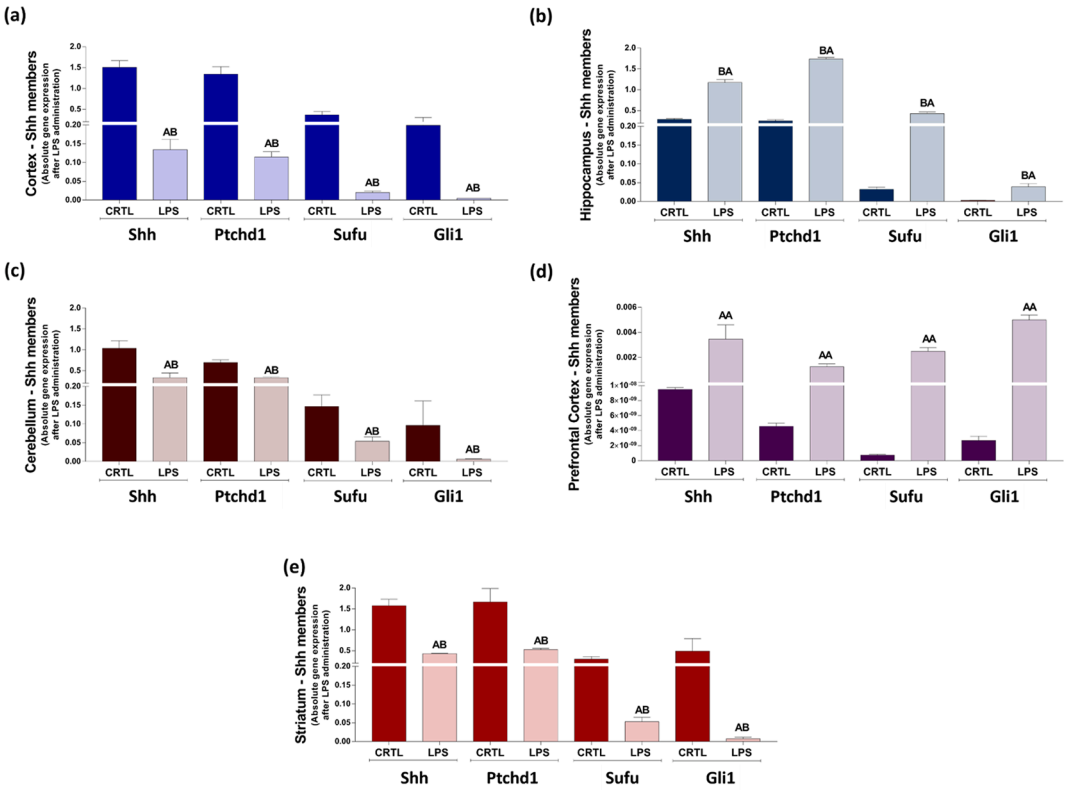

Fig. 7. Effect of Neuroinflammation on relative gene expression of Hedgehog pathway components. The gene expression of Hedgehog pathway components [Sonic Hedgehog (*Shh*), Patched 1 (*Ptchd1*), Oncogene Homolog fusion suppressor (*Sufu*) and Glioma-Associated 1 (*Gli1*)] were evaluated by reactions of qPCR in the Cortex (CTX) (a), Prefrontal Cortex (PFC) (b), Cerebellum (CRB) (c), Hippocampus (HIP) (d) and Striatum (STR) (e) after 24 h of LPS administration (0.33 mg/kg). The *Gapdh*, *β-actin* and *18 s* genes were used as normalizers. The results were calculated using the method ($2^{-\Delta Ct}$) and represent the mean ± standard deviation of 5 independent animals performed in technical duplicate and shown in a graphical format with normalized values as a function of the control assigned value of 1. Different letters indicate a statistically significant difference. Capital letters compare groups with and without LPS within each analyzed region.

A more in-depth analysis was performed between the expression of the Hedgehog members and their promoter methylation status, to test their correlation (Fig. 6b, d, f, **h**). The DNA hypomethylation observed in the *Ptchd1* in all analyzed brain regions (Fig. 6**i-m**) reflected in a transcriptional activation only in CRB, PFC and CTX (Fig. 6d). Correlations with a Pearson product moment above $r \geq 0.6$ were observed for the *Shh* gene in the STX, HIP, CRB and CTX (Fig. 6b); for the *Ptchd1* in CRB, PFC and CTX (Fig. 6d); for *Sufu* in the HIP, CRB and PFC (Fig. 6f) and for *Gli1* in the STR, HIP and PFC (Fig. 6h). These results of mRNA levels being inversely proportional to the DNA methylation status suggest methylation mechanism may be one of the driving forces responsible for the transcriptional profile of Hedgehog members in the brain regions analyzed.

2.3. Neuroinflammation increased the gene expression of Hedgehog pathway members in HIP

To identify whether neuroinflammation modulated the transcripts of the Hedgehog pathway members in different brain regions, we evaluated their gene expression 24 h after intraperitoneal administration of LPS. As shown in Fig. 7, brain regions responded differently to neuroinflammation. The expression of *Shh*, *Ptchd1*, *Sufu* and *Gli1* genes was down-regulated in CTX (Fig. 7a), CRB (Fig. 7c) and STR (Fig. 7e) and up-regulated in HIP (Fig. 7d). In detail, the highest levels of the ligand *Shh* and the receptor *Ptchd1*, were triggered in HIP, after neuroinflammation was induced. It is interesting to note the HIP is the structure that presented the highest absolute gene expression values of all members, while and the PFC showed the lowest values (Fig. S1a-d).

Afterwards, we compared each Hedgehog pathway members in each brain structure and showed *Shh* and *Ptchd1* presented similar patterns comparing the brain regions analyzed, with high gene expression of *Sufu* and *Gli1* in HIP. The PFC presented the lowest levels of transcripts of all Hedgehog pathway members (Fig. S1a-d). Additionally, when the Hedgehog pathway members were evaluated in the same brain region, a similar pattern among CRB, HIP and STR was observed, with highest levels of *Shh* and *Ptchd1* and lowest levels of *Sufu* and *Gli1* (Fig. S1g-**i**). There was no modulation in the PFC while *Ptchd1* presented high gene expression levels in the CTX (Fig. S2e, f). All the above described results can also be observed with statistical details in the Table S2.

2.4. Region-specific modulation of epigenetic machinery by the inflammatory response in the CNS

The gene expression profile of the DNA methylation-modifying enzymes was performed to better clarify the gene regulation in different brain regions, in response to neuroinflammation. The DNA methylation-modifying enzymes expression was distinct, regardless of family (*Dnmts* or *Tets*) and brain region, after the treatment with LPS (Fig. 8a-f). The analyses did not show any statistical differences for *Dnmts* in all brain regions (Fig. 8a, c, e, **g, i**) while all *Tets* decreased in the CTX and STR (Fig. 8**b, j**). There was no modulation in PFC and CRB (Fig. 8d, f**),** with increase in the *Tet2* transcripts in the HIP (Fig. 8**h**). When all brain regions were compared, the PFC showed the lowest levels while HIP demonstrated the highest levels of all *Dnmts* and *Tets* (**Fig. S3a-f**). However, when the gene expression patterns of *Dnmts* and *Tets* are compared in each brain region, the results shown in Fig. S4a-e demonstrated there is a tendency of DNA hydroxymethylation only for STR and HIP regions, characterized by high levels of *Tet2* and Tet methylcytosine dioxygenase 3 (*Tet3*) transcripts.

The statistical analysis demonstrated significant statistical

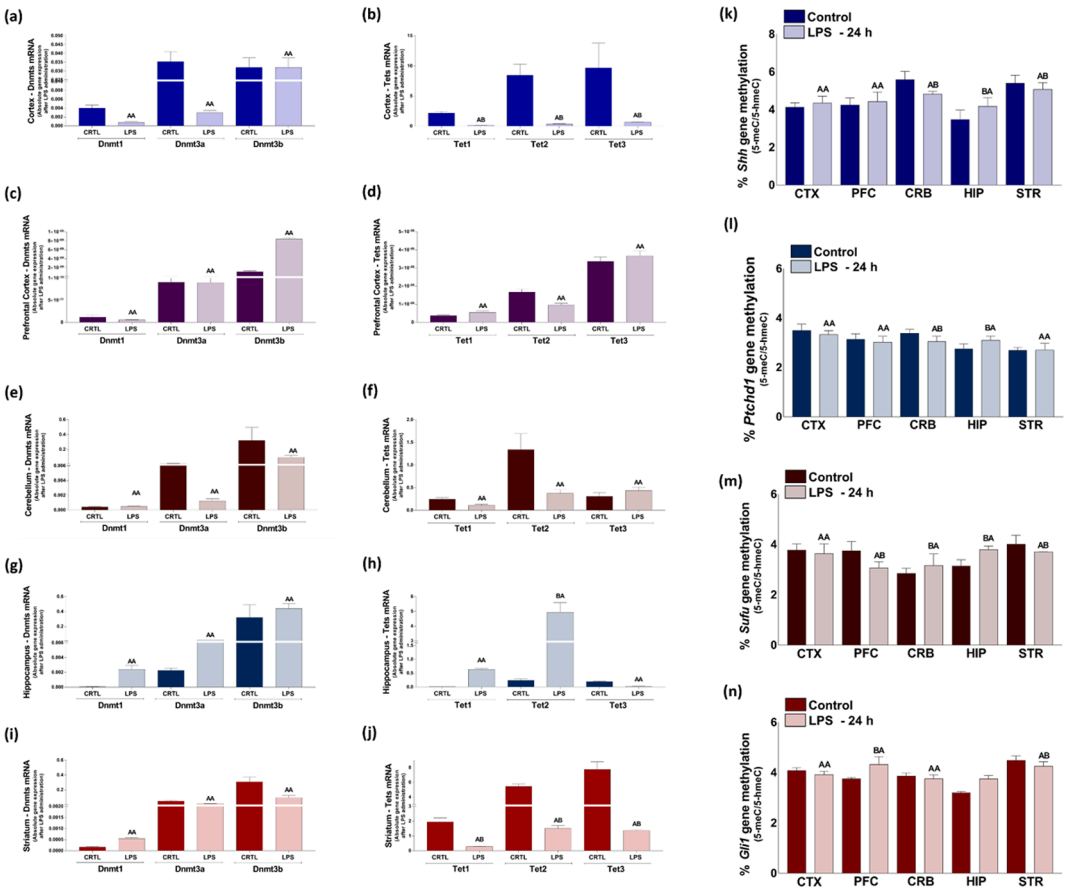

Fig. 8. Neuroinflammation impact on the epigenetic landscape of Hedgehog pathway components. The gene expression of DNA methylation-modifying enzymes and the methylation status of the promoter region of the Hedgehog members were evaluated in brain structures after 24 h of intraperitoneal administration of LPS (0.33 mg / kg). The DNA methyltransferases (Dnmt1, Dmnt3a and Dnmt3b) and DNA demethylases (Tet1, Tet2 and Tet3) gene expression in the Cortex – CTX (a,b), Prefrontal Cortex - PFC (c,d), Cerebellum – CRB (e,f), Hippocampus – HIP (g,h) and Striatum – STR (i,j) was determined by qPCR after RNA extraction using the TRIzol® method after 24 h of LPS administration (0.33 mg/kg). Gene promoter hydroxymethylation/methylation patterns were investigated by DNA glycosylation by T4-BGT and *Msp*I and *Hpa*II digestion followed by qPCR analysis with specific primers. The DNA methylation status of the Hedgehog members [Sonic Hedgehog – *Shh* gene (l), Patched 1 – *Ptchd1* gene (m), Oncogene Homolog fusion suppressor – *Sufu* gene (n), Glioma-Associated 1 – *Gli1* gene (n). The relative methylation levels were presented as a 5-mec/5hmec ratio and determined using the cycle threshold (Ct) method and the methylation results are presented as Ct [*Hpa*II] – Ct [*Msp*I] /Ct [SE] and the hydroxymethylation results are presented as Ct [*Msp*I] Ct [SE]. Results were represented as mean ± standard deviation of 5 independent animals performed in technical duplicate. Different letters indicate a statistically significant difference. Capital letters compare groups with and without LPS within each analyzed region.

differences for group (F = 174.45; p = 0.000), region (F = 107.07; p = 0.000) and DNA methylation-modifying enzymes (F = 159.19; p = 0.000) factors. There was double interaction between group/region (F = 115.41; p = 0.000), group/DNA methylation-modifying enzymes (F = 35.54; p = 0.000) and triple interaction between group/region/DNA methylation-modifying enzymes (F = 33.74; p = 0.000). The unfolding of the triple interaction was performed by the Bonferroni adjusted test (**Table S3**).

2.5. Neuroinflammation modifies the epigenetic landscape of the Hedgehog pathway components

Considering the specific transcript profiles of the DNA methylation-modifying enzymes and the high expression of *Tets*, we evaluated whether the Hedgehog pathway members were epigenetically modified in response to neuroinflammation. To this end, the genomic DNA was previously digested by methylation-sensitive endonucleases and subsequently amplified with specific primers flanking DNA regulatory regions, with at least one recognition site for restriction enzymes (CpG site). The epigenetic analysis of the Hedgehog pathway members showed modulation in the DNA (hydroxy)methylation patterns in their promoters, except in the CTX region. The PFC showed no differences for *Shh* and *Ptchd1*, with DNA hypomethylation in *Sufu* and DNA hypermethylation in *Gli1* promoters. DNA hypomethylation was observed in *Shh* and *Ptchd1*, with DNA hypermethylation in *Sufu* in the CRB. On the other hand, we observed a DNA hypermethylation in *Shh, Ptchd1* and *Sufu* promoters in HIP, while DNA hypomethylation of *Shh*, *Sufu* and *Gli1* promoters was observed in the STR (Fig. 8**k-n**). The DNA methylation levels were compared between the Hedgehog pathway members, in each one of the brain regions analyzed here. The results showed the *Shh* was the most methylated member while *Ptchd1* was the less methylated one (**Fig. S5**). These results can also be observed with statistical details in the **Table S4**.

In order to test whether the epigenetic changes promoted by neuroinflammation were directly related to the changes observed in the gene expression of the Hedgehog pathway members, we used the Pearson correlation test between DNA methylation and gene expression. Correlations with a Pearson product moment above r ≥ 0.6 were observed for the *Shh* in the CRB (Fig. S6c), *Ptchd1* in the HIP (Fig. S6i), *Sufu* in the PFC (Fig. S6l) and HIP (Fig. S6n) and *Gli1* in the CTX (Fig. S6p) and STR (Fig. S6t). However, only for the *Sufu* gene in the PFC the mRNA levels were inversely proportional to the DNA methylation of the promoter region, suggesting DNA methylation as one of the mechanisms involved in the transcriptional regulation (Fig. S6l).

The statistical analysis showed significant statistical differences for group ($F = 174.45$; $p = 0.000$), region ($F = 107.07$; $p = 0.000$) and DNA methylation-modifying enzymes ($F = 159.19$; $p = 0.000$) factors. There was double interaction between group/region ($F = 115.41$; $p = 0.000$), group/DNA methylation-modifying enzymes ($F = 58.68$; $p = 0.000$), region/DNA methylation-modifying enzymes ($F = 35.54$; $p = 0.000$) and triple interaction between group/region/DNA methylation-modifying enzymes ($F = 33.74$; $p = 0.000$) factors. The unfolding of the triple interaction was performed by the Bonferroni adjusted test (**Table S4**).

3. Discussion

The involvement of the Hedgehog (Hh) signaling pathway, by which SHH is the main activating ligand in the brain, is central to the development and standardization of the CNS during embryogenesis (Charytoniuk et al., 2002; Petrova and Joyner, 2014), acting actively in the coordination of diversification, standardization, growth and differentiation of the vertebrate nervous system (Placzek and Briscoe, 2018). Even though the additional functions of SHH in post-embryonic brains are in focus, some questions about the abundance of endogenous SHH and its changes over time in post-embryonic and mature brains (Rivell et al., 2019) are still poorly understood, including its function during neuroinflammation. To better elucidate its involvement during neuroinflammation, the neuroinflammatory profile after intraperitoneal administration of LPS at one dose (0.33 mg/kg) was initially characterized by evaluating the gene expression of inflammatory cytokines in different regions of the brain. It should be noted that this dose has been widely used by different research groups, and its behavioral, biochemical and molecular effects are widely known (Hoogland et al., 2015; Scheffer et al., 2019; Vichaya et al., 2019). We know that peripheral injections of LPS did not penetrate in the CNS; instead, this administration induces the expression of proinflammatory cytokines in the brain and have profound depressing effects on spontaneous and learned behaviors (Dunn, 2006). Some studies have reported after 24 h of LPS administration, rodents developed behaviors related to depressive states accompanied by an important neuroinflammatory state (Biesmans et al., 2013; Millett et al., 2019).

Acute systemic LPS administration induces several behavioral, immune, and hormonal effects called sickly behavior. Sickness behavior is a coordinated set of adaptive behavioral changes that occur in physically ill animals and humans during infection. These behaviors include lethargy, depressed mood, reduced social exploration, loss of appetite, sleepiness, hyperalgesia, and, at times, confusion. This set of behaviors often accompanies fever and is considered a motivational state responsible for reorganizing an ill individual's perceptions and actions to enable better coping with infection (Dantzer et al., 2008). In our study, a reduced rearing and grooming frequencies without interferences with locomotion distance were observed. In addition, the immobility time and its frequency were increased. In this respect, we investigated, previously, the temporal effects of LPS (100 μg/kg) on sickness behavior of virgin and lactating female rats (Nascimento et al., 2013). At two hours after LPS, the most effect observed in the virgin females treated with the LPS was a decreased tympanic temperature. At 48 h after the endotoxin administration the tympanic temperature increased, the food consumption and body weigh decreased. At 72 two h after the LPS administration all parameters of the females treated with LPS were like those of the control group. Thus, LPS induced several signs of sickness behavior until 48 h after administration. In the present study, despite the mice were observed 24 h after the LPS administration, we could observe clear signs of sickness behavior, as the reduced rearing and grooming behavior associated with increased immobility. We attributed these results to the high dose used in our experiment revealing that, even after 24 h after endotoxin administration, the animals showed signs of sickness behavior.

The changes observed in the gene expression of pro and anti-inflammatory cytokines in the different brain regions confirmed the relevant effects of LPS, even after 24 h of its administration, validating our experimental model. After 24 h, the CTX, PFC and HIP were the brain areas most affected by the treatment with LPS, based on the comparing the gene expression of all inflammatory cytokines evaluated in this study within the same brain region. We know that the behavioral dysfunction normally seen in animal models stimulated by LPS correlates with elevated levels of proinflammatory cytokines and oxidative stress parameters in the HIP (Zhao et al., 2019), PFC (Noh et al., 2014), CRB and other brain regions (Abg Abd Wahab et al., 2019). This information is in accordance with our results that demonstrated an imbalance between the cytokines gene expression and both increased serum and hippocampal concentrations of pro-inflammatory cytokines.

The Hedgehog pathway is fundamental for the maintenance of neuronal activity proliferation of neural stem cells and anti-inflammatory action, especially in adult brains (Pérez-Domínguez et al., 2018). Therefore, to better characterize the transcriptional panorama of the main members of the Hedgehog pathway, we first characterized their transcriptional profile and methylation status in the promoter region, at basal levels. Based on the results obtained in this step, we found the differential gene expression profile of the Hedgehog pathway members observed between different brain regions is strongly influenced by DNA methylation. It has previously been shown that the components of this pathway are widely expressed throughout the adult anterior brain parenchyma (Traiffort et al., 1999). The results presented here demonstrated that the PFC is the region with the lowest absolute values of the Hedgehog pathway members (*Shh*, *Ptchd1*, *Sufu*), which suggest less activity of the PFC. On the other hand, the overexpression of striatal *Gli1* highlights the importance of this pathway for this region in particular, since it has already been demonstrated that *Gli1* is expressed in cells responsive to *Shh* (Marigo et al., 1996; Sasaki et al., 1997). It is noteworthy that *Gli1* actively participates in the renewal of cancer stem cells and the combined use of SHH signaling inhibitors with immunotherapy, radiation therapy and chemotherapy is the key point for treating these cells (Lee et al., 2012; Jeng et al., 2020).

In adulthood, we know SHH actively participates in the control of vascular proliferation, neurogenesis and tissue repair in the CNS (Petrova and Joyner, 2014) and its absence is associated with a midline defect, holoprosencephaly, spina bifida and exencephaly (Murdoch and Copp, 2010). It is noteworthy that we characterized here, for the first time, the epigenetic involvement in determining the endogenous abundance of the *Shh* ligand and other components of the Hedgehog pathway in the adult brain.

It is true that epigenetic changes, such as DNA methylation, are commonly detected as mechanisms responsible for the transcriptional control of Hedgehog pathway members (Wils and Bijlsma, 2018). In addition, we know that the DNA methylation pattern is determined mainly by the dynamics of the two classes of enzymes, DNMTs and TETs. DNMTs are divided into two classes: the maintenance methylases represented by DNMT1 and the *de novo* methylases, DNMT3a and DNMT3b, responsible for the methylations that occur without the presence of previous methylation (Cui and Xu, 2018). Our study showed an inversely proportional correlation between endogenous expression and the DNA methylation status of the promoter region of the *Shh* genes except for PFC; *Ptchd1* (except for STR and HIP); *Sufu* (except for STR and CTX) and Gli1 (except for CRB and CTX). These results reinforce the hypothesis that the differential expression of DNA-modifying enzymes, especially the high basal expression of *Tets* in the different regions is related to the DNA hypomethylation, observed in the promoter region in the adult brain. It should be noted that the similar transcriptional profile of *Dnmt1* observed between the structures and the reduced endogenous levels of *Dnmt3a* is in line with published studies. These previous publications showed that due to DNMT1 role in maintenance of DNA methylation patterns in dividing cells, it is crucial the expression of DNMT1 in the constant post-mitotic state in the brain (Edwards et al., 2017; Jurkowska et al., 2011). DNMT3a, on the other hand, seems to be

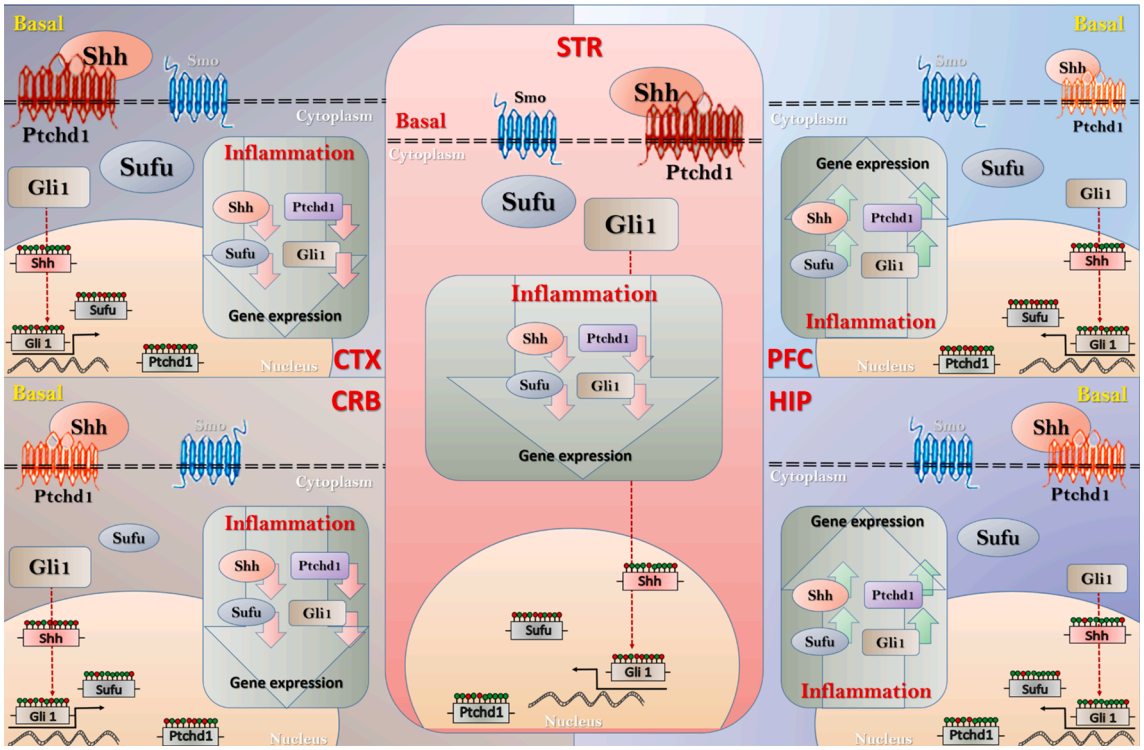

Fig. 9. Graphical abstract. Representation of gene expression and DNA methylation profiles of the Sonic Hedgehog pathway members in the adult brain (Basal) and the impact of neuroinflammation on the transcriptional landscape of components of the Hedgehog pathway (Inflammation). Different gene expression levels at Basal were represented by different size of letters of the gene symbols: [Sonic Hedgehog (Shh), Patched 1 (Ptchd1), Oncogene Homolog fusion suppressor (Sufu) and Glioma-Associated 1 (Gli1*)*. In the group in which LPS-induced Neuroinflammation, the impact of inflammation on the transcriptional profile was represented by arrows, being for up-regulation and for down-regulation. Brain regions: Cortex (CTX), Prefrontal Cortex (PFC), Cerebellum (CRB), Hippocampus (HIP) and Striatum (STR).

more necessary during the initial postnatal phases, in which it is shown with high expression, being drastically reduced in cortical neurons in the adult phase (Wilson et al., 1987).

The regulation of DNA methylation in the adult brain is still uncertain and in constant discovery. Although the 5-methylcytosine (5-meC) mark has been considered a stable feature, the conversion of 5-meC to 5-Hydroxymethylcytosine (5-hmeC) by the action of TETs enzymes has gained increasing prominence in neural processes (Bhutani et al., 2011). Thus acting in the opposite direction, we have the action of TET proteins, responsible for the conversion of 5-meC into 5-hmeC and subsequent formation of 5-formylC and 5-carboxycyl, important intermediates of DNA demethylation processes (Pfeifer et al., 2013). In this scenario, it is important to note that our results showed *Tet2* and *Tet3* as the most expressed enzymes in all brain regions, with baseline values significantly higher than the *Dnmts*. These results are in accordance with a study by Szwagierczak and collaborators, published in 2010, that characterized the enzyme TET3 as the member of the TET family most abundant in the CRB and HIP (Szwagierczak et al., 2010). On the other hand, the high expression of *Tet2* in the CRB is still a finding that needs to be better investigated. What is certain is that TET2, unlike TET1 and TET3, mainly regulates the levels of 5-hmeC in gene bodies and not in promoters (Williams et al., 2011); in addition, TET2 seems to be related to rescuing the cognitive decline related to age, preserving adult hippocampal neurogenesis (Gontier et al., 2018). However, due to the limited number of studies regarding the function of TET2, specifically in the CRB, our conclusions are limited.

In this study, in addition to demonstrating that the epigenetic control of Hedgehog pathway members is region-specific, we also examined the impact of the LPS-induced acute neuroinflammation on this signaling pathway. In particular, the results of *Dnmts* gene expression analysis indicate the HIP was the most susceptible brain structure to changes in gene expression, after the neuroinflammatory induction. A significant increase was observed for all *Dnmts*, corroborating some previous results that demonstrated the expression of DNMTs was affected by the injection of LPS IP in adult rats (Matt et al., 2018). It is true that changes in the expression of DNMTs can provide mechanistic support for changes in DNA methylation observed in gene promoter regions associated with neural plasticity (Boersma et al., 2014) and the inflammatory response (Matt et al., 2018). On the other hand, it has been shown that inhibition of DNMT1 has impact on recovered memory consolidation with a concomitant increase in the expression of synaptic plasticity genes, such as the brain-derived neurotrophic factor (BDNF) (Singh et al., 2015). Activation of Shh receptors accelerates axonal growth and release of glutamate from presynaptic endings. However, if the Shh signaling is not working properly, might affects the HIP, leading to changes in the plasticity of neuronal circuits and in axonal degeneration and impairment of memory and learning (Yao et al., 2016).

For epigenetic regulators responsible for DNA hydroxymethylation and influence on DNA demethylation (Kohli and Zhang, 2013), our results showed that only the expression of *Tet2* in the HIP and *Tet3* in the CRB was positively regulated by neuroinflammation. These results are opposed to other results that showed LPS decreased *Tet1* and increased *Tet2*, without any effect on *Tet3*, in the microglia collected after 4 h of Intracerebroventricular (ICV) injections of LPS in adult mice (Matt et al., 2018). Noteworthy, it has recently been shown that *Tet2* regulates the proinflammatory response in the microglia of mice injected intraperitoneally with LPS. In addition, this expression was increased in the microglia by different inflammatory agents, through an Factor Nuclear Kappa B (NF-Kb)-dependent pathway, promoting transcriptional modifications leading to early metabolic changes, as well as a later inflammatory response, regardless of the activity of DNA demethylases (Carrillo-Jimenez et al., 2019).

In this sense, we hypothesize that the reduction in the *Tet3* expression in the CTX, HIP and STR along with its increase in the CRB promoted by neuroinflammation, might be related to specific functions of each brain region, since *Tet3* is highly expressed in the brain, mainly in neurons and oligodendrocytes, and absent in astrocytes, being considered as a synaptic sensor, capable of regulating neuronal activity (Yu et al., 2015). Studies of ablation of TET3 in mature adult neurons promoted dysregulation of genes involved in the glucocorticoid signaling pathway (HPA axis) in the ventral HIP concomitant with anxiolytic behavior and impaired spatial orientation (Antunes et al., 2021). In addition, TET3 is involved in controlling the differentiation (Montalbán-Loro et al., 2019) and identity (Santiago et al., 2020) of Neural Stem Cells and their negative regulation can reduce global levels of 5-hmeC and promote tumorigenesis of glioblastoma (Carella et al., 2020). Surprisingly, all this changes in the transcriptional profile of DNA-modifying enzymes were able to promote significant changes in the DNA methylation status of the promoter region of Hedgehog pathway members. Here, the changes in the DNA methylation status did not have an inversely proportional correlation with the gene expression patterns after the induction of neuroinflammation, suggesting distant promoters or enhancers might be also involved in the fine-tuning of transcriptional regulation during neuroinfammation or that relevant CpGs were not targeted in the present analysis.

The present study was designed to characterize the link between DNA methylation and transcription control of the Hedgehog pathway members, and the impact of acute neuroinflammation on this process. We hypothesized the administration of LPS in adult rats would promote changes in the DNA methylation-modifying enzymes with changes in the transcriptional profile of the Hedgehog pathway members. A particularly interesting finding was that Hedgehog pathway members responded homogeneously to neuroinflammation, independent of the brain region. Among the numerous functions associated with this pathway in the adult brain, recent findings suggest an important role in maintaining blood–brain barrier (BBB) integrity; in addition, its deregulation could contribute to neuropathogenesis of neurodegenerative diseases such as Alzheimer's and Parkinson's disease, and amyotrophic lateral sclerosis (Yang et al., 2021; Bohannon et al., 2019).

Altogether, our results (Fig. 9) support the hypothesis that epigenetic mechanisms, such as DNA methylation, might be involved in determining the endogenous expression pattern of Hedgehog pathway members, in the adult brain. In addition, the acute neuroinflammation modulates both gene expression of DNA-modifying enzymes and the Hedgehog pathway members, but only the reduction in *Sufu* gene expression was accompanied by increased DNA methylation levels of the promoter region. Despite the mechanistic limitations, this study points to DNA methylation as the mechanism responsible for determining the endogenous transcriptional profile of the Hedgehog pathway members, expanding the current knowledge on the mechanisms associated to the differential transcriptional profile of its members, among brain regions. Given the evolutionarily conserved role of the Hedgehog pathway during neurodevelopment, along with recent reports of the beneficial effect of Shh on the adult brain, it is logical to think that increased expression of members of this pathway might be an adaptive host response to acute inflammation. On the other hand, reports in the literature have related the prolonged increase in Shh with the development of brain tumors (Northcott et al., 2019). These data demonstrated the dichotomous nature of this pathway, having acute protective effects, although detrimental effects can be observed with prolonged activation. Consistent with the notion of the Hedgehog pathway acting temporarily, our study demonstrates that neuroinflammation promotes the transcriptional repression of the *Sufu* gene, responsible for the cytoplasmic sequestration of the transcription factor Gli1 (Doheny et al., 2020). Despite the evidence presented in our study suggesting that activation of the Hedgehog pathway by neuroinflammation has beneficial effects, further investigation is needed, especially in contexts of chronic neuroinflammation. Therefore, the data presented here opens a new avenue of possibilities and future research should be carried out to better understand this signaling pathway, which has great potential not only for the treatment of brain tumors, but for the development of numerous neurodegenerative diseases that have neuroinflammation as common component in their pathophysiology.

4. Experimental procedure

4.1. LPS-induced neuroinflammation

Neuroinflammatory response was induced in adult male Swiss mice aged 3 to 5 months and body mass ranging between 45 and 50 g by the administration of a single intraperitoneal (i.p.) injection of Escherichia coli lipopolysaccharide (LPS; E. coli LPS, 0.33 mg/kg, serotype 0127: B8). Control animals received vehicle injections (saline; i.p.). The dosage of 0.33 mg/kg of LPS was selected based on previous results from our research group in which different studies showed that a single dose of LPS at this concentration was able to induce neuroinflammation in the brain of adult mice with behavioral changes, proven biochemical and molecular (Henry et al., 2009; Ghisoni et al., 2015; de Paula Martins et al., 2018). The experiments were conducted in accordance with the National Research Council's Guidelines for the Care and Use of Laboratory Animals and approved by the Local Ethical Committee.

4.2. Cytokine production

The simultaneous detection of Il 2, Il 4, Il 6, Il 10, Il 17, Ifn-γ, and Tnf-α cytokines in serum and hippocampal lysates were done using mouse Th1/Th2/Th17 cytometric bead array (CBA) kit (BD Bioscience, CA, USA), according to the manufacturer's instructions. Briefly, 25 μL of each sample were incubated with 25 μL of capture beads conjugated to allophycocyanin (APC) and 25 μL of phycoerythrin (PE)-conjugated detection antibodies, for 2 h at room temperature in the dark. After this, samples were washed and resuspended in the same buffer for data acquisition using Accuri™ C6 flow cytometer (BD Bioscience, USA). Data analysis was performed using the analysis software FCAP Array v3.0.1 (BD Biosciences) and graphs were done using GraphPad Prism 7.0. Values were expressed in pg/mL, considering the limit of detection for each cytokine provided by the manufacturer.

4.3. Behavioral tests

The open-field test is used to evaluate motor/exploratory and anxiety-like The device is round with 40 com diameter and 30 cm height, painted white. The test room was small and with dim lighting, isolated from the experimenter. The locomotion and rearing frequencies, the grooming time (s), the grooming frequency, the time of immobility (s) and its frequency were assessed during 3 min. A video camera mounted 100 cm above the arena collected the data to posterior analysis. The apparatus was cleaned with a 5 % alcohol/water solution before placement of the mouse to obviate possible biasing effects from odor cues left by previous mouse (Kirsten et al., 2022).

4.4. qPCR gene expression analysis

Total RNA was isolated from different brain structures 24 h after LPS administration using the TRIzol1/chloroform/isopropanol method (Invitrogen, Carlsbad, CA, USA). The quantity and purity of extracted RNA was estimated by using the spectrophotometer apparatus NanoDrop, at 260 and 280 nm. Previously, 2000 ng of total RNA was used for cDNA synthesis with Superscript II (Invitrogen, Carlsband, CA, USA) according to manufacturer's instructions. qPCR analysis was performed using SYBR Green Master Mix (PowerUp™ SYBR™ Green Master Mix - Applied Biosystems, Foster City, CA, USA). All the reactions were carried out in a total of 10 μL, containing 5 μL, specifics primers (0.5 μM), 50 ng of cDNA and nuclease free H_2O in a QuantStudio® 3 Real-Time PCR

Table 1
Expression primers sequences and PCR cycle conditions.

Gene (ID)	Primer	5′- 3′ Sequence	Reactions Condicition	Product size
Rn 18 s (19791)	Forward	CGC GGT TCT ATT TTG TTG GT	95 °C – 15 s; 60 °C – 30 s; 72 °C – 30 s	179
	Reverse	TCG TCT TCG AAA CTC CGA CT		
β-actin (11461)	Forward	TCT TGG GTA TGG AAT CCT GTG	95 °C – 15 s; 58 °C – 30 s; 72 °C – 30 s	82
	Reverse	AGG TCT TTA CGG ATG TCA ACG		
Gapdh (14433)	Forward	CCG CAG CGA GGA GTT TCT C	95 °C – 15 s; 63 °C – 30 s; 72 °C – 30 s	530
	Reverse	GAG CTA AGC TCA GGC TGT TCC A		
Dnmt1 (13433)	Forward	CCT TTG TGG GAA CCT GGA A	95 °C – 15 s; 63 °C – 30 s; 72 °C – 30 s	178
	Reverse	CTG TCG TCT GCG GTG ATT		
Dnmt3a (13435)	Forward	GAG GGA ACT GAG ACC CCA C	95 °C – 15 s; 63 °C – 30 s; 72 °C – 30 s	216
	Reverse	CTG GAA GGT GAG TCT TGG CA		
Dnmt3b (13436)	Forward	AGC GGG TAT GAG GAG TGC AT	95 °C – 15 s; 63 °C – 30 s; 72 °C – 30 s	72
	Reverse	GGG AGC ATC CTT CGT GTC TG		
Tet1 (52463)	Forward	GAG CCT GTT CCT CGA TGT GG	95 °C – 15 s; 65 °C – 30 s; 72 °C – 30 s	202
	Reverse	CAA ACC CAC CTG AGG CTG TT		
Tet2 (214133)	Forward	AAC CTG GCT ACT GTC ATT GCT CCA	95 °C – 15 s; 65 °C – 30 s; 72 °C – 30 s	182
	Reverse	ATG TTC TGC TGG TCT CTG TGG GAA		
Tet3 (193348)	Forward	GTC TCC CCA GTC CTA CCT CCG	95 °C – 15 s; 58 °C – 30 s; 72 °C – 30 s	136
	Reverse	GTC AGT GCC CCA CGC TTC A		
Shh (20423)	Forward	AGC GAC TGC GAA ATA AGG AA	95 °C – 8 s; 59 °C – 8 s; 72 °C – 8 s	234
	Reverse	GCC AGG AGA GGA GAA AAA CA		
Sufu (24069)	Forward	TGA AAA GAT GCT TGG TGC TG	95 °C – 15 s; 60 °C – 30 s; 72 °C – 30 s	155
	Reverse	TCC CCA GAG CCT TGT AGA GA		
Patch 1 (19206)	Forward	TGT GTG CAT GTG ACT TTC CA	95 °C – 15 s; 60 °C – 30 s; 72 °C – 30 s	152
	Reverse	CCA GCA TCA CGA CAG AAA AA		
Gli 1 (14632)	Forward	GAA GGA ATT CGT GTG CCA TT	95 °C – 15 s; 59 °C – 8 s; 72 °C – 8 s	148
	Reverse	GCG TCT TGA GGT TTT CAA GG		
Il1β (16176)	Forward	GAC CTT CCA GGA TGA GGA CA	95 °C – 15 s; 60 °C – 30 s; 72 °C – 30 s	183
	Reverse	AGC TCA TAT GGG TCC GAC AG		
Il6 (16193)	Forward	AGT TGC CTT CTT GGG ACT GA	95 °C – 15 s; 60 °C – 30 s; 72 °C – 30 s	191
	Reverse	CAG AAT TGC CAT TGC ACA AC		
Il 10 (16153)	Forward	CCA AGC CCT TAT CGG AAA TGA	95 °C – 15 s; 60 °C – 30 s; 72 °C – 30 s	163
	Reverse	TTT TCA CAG GGG AGA AAT CG		
Il 13 (16163)	Forward	CAG TCC TGG CTC TTG CTT G	95 °C – 15 s; 60 °C – 30 s; 72 °C – 30 s	165
	Reverse	CCA GGT CCA CAC TCC ATA CC		
Il 18 (16173)	Forward	ACT TTG GCC GAC TTC ACT GT	95 °C – 15 s; 60 °C – 30 s; 72 °C – 30 s	125
	Reverse	GGG TTC ACT GGC ACT TTG AT		
Il 33 (77125)	Forward	CCT TCT CGC TGA TTT CCA AG	95 °C – 15 s; 60 °C – 30 s; 72 °C – 30 s	187
	Reverse	CCG TTA CGG ATA TGG TGG TC		
Tnf-α(21926)	Forward	CCA CAT CTC CCT CCA GAA AA	95 °C – 15 s; 60 °C – 30 s; 72 °C – 30 s	259
	Reverse	AGG GTC TGG GCC ATA GAA CT		

(Thermo Fisher Scientific, Waltham, Massachusetts, USA). Gene expression was expressed as compared to control cells by $^{\Delta\Delta}$CT method, using the average of the *Gapdh*, *β-actin* and *18 s* genes as normalizers. The primers (Exxtend, Campinas, SP, Brazil) sequence and PCR conditions were expressed in Table 1.

4.5. Genomic DNA extraction

The DNA genomic was extracted of different brain structures 24 h after LPS administration using the using the classic phenol–chloroform method (Toni et al., 2018). Simply, each specimen was gently poured into a 1.5 mL Eppendorf tube and centrifuged at 12.000 rpm for 10 min. The supernatants were completely removed and obtained pellets were mixed with 150 μL of lysing buffer followed by incubation at 80 °C for 20 min. Proteinase K was added and finally the mixture was heated at 56° C for 30 min. Next, only 50 μL of neutralizing buffer was added to the mixture. Also, 200 μL of equilibrium phenol was transferred to the tube and thus the mixture was spun down at 5000 rpm for 10 min. The upper aqueous layer containing the target DNA was preserved and mixed with 200 μL of chloroform and 20 μL of sodium acetate. The mixture was centrifuged at 12.000 rpm for 10 min. Then, 120 μL of isopropanol was added to the mixture and incubated overnight. Next, the mixture was centrifuged at 12000 rpm for 10 min at 4 °C. The supernatant was removed and an aliquot of 200 μL of 70 % alcohol was poured into the tube and centrifuged at 12.000 rpm for 4 min at 4 °C. The supernatant was completely discarded and 50 μL of distilled water (DW) was added to the tube.

4.6. Promoter DNA methylation

For 5-methylcytosine (5-meC) and 5-hydroxymethylcytosine (5-hmeC) analysis content, initially the same concentration of genomic DNA was treated with T4-β-glucosyltransferase (T4-BGT - New England BioLabs, Beverly, MA), that adds glucose moiety to 5-hmeC (gDNA) to distinguish between DNA methylation and hydroxymethylation. Subsequently, the samples were digested with *Msp*I or *Hpa*II restriction enzymes (New England BioLabs, Beverly, MA). After DNA treated the qPCR reactions was carried in 40 cycles of amplification out in a total of 10 μL, containing PowerUp™ SYBR™ Green Master Mix 2 × (5 μL; Applied Biosystems, Foster City, CA), 0.5 μM of each primer, 1 μL of treated gDNA and nuclease free H_2O. The primers were designed on regulatory regions (DNaseI hypersensitivity clusters sites, layered by histone modifications marks, CpG regions and transcription factors binding sites) using Primer3 Input (version 0.4.0) software. The primers were blasted using in-silico PCR (https://genome.ucsc.edu/) and the characteristics of primers and regions of genes analyzed and PCR conditions are illustrated in Table 2 **and** Fig. 1 The 5-meC or 5-hmeC levels were determined using the cycle threshold (Ct) method and the methylation results are presented as *Hpa*II levels - *Msp*I levels/Control

Table 2
Methylation primers sequences and PCR cycle conditions.

Gene (ID)	Primer	5′- 3′ Sequence	Reactions Condicition	Product size	CpG Island Location
Shh (20423)	Forward Reverse	AGG AAG GTG AGG AAG TCG CT CAC ACA CAC ACG CTC GTA CA	95 °C –15 s; 60 °C – 30 s; 72 °C – 30 s	244	chr 4 28784319–28785746 (site 5)
Ptch1 (19206)	Forward Reverse	GGA TCC CAA GGA GGA AGA AG ATG GCC TCG GCT GGT AAC	95 °C –15 s; 60 °C – 30 s; 72 °C – 30 s	217	chr 13 63664549–63667490 (site6)
Sufu (24069)	Forward Reverse	CTC TAC CCT CCC GGG TTC T GAC GAT AGC GGT AAC CTG GA	95 °C –15 s; 60 °C – 30 s; 72 °C – 30 s	214	chr 19 46450187–46450655 (site 4)
Gli (14632)	Forward Reverse	CTC ATC CTC CTC ACA GCC GCA CTG GGC AGC AAC ACC TCC CA	95 °C –15 s; 60 °C – 30 s; 72 °C – 30 s	380	chr 10 127339344–127339723 (site 5)

levels and the hydroxymethylation results are presented as *Msp*I levels-Control levels.

4.7. Statistical analysis

Gene expression and promoter DNA methylation results are expressed as mean ± standard deviation of 5 animals and were performed in technical duplicate. Based on the experimental design of variables, gene expression (inflammatory cytokines, DNA methylation-modifying enzymes and Sonic Hedgehog Pathway Members) and methylation of the promoter region of Sonic Hedgehog Pathway Members, which were measured in different brain regions (CTX, PFC, CRB, HIP and STR) within the same rat and in different groups [without LPS (Control) and with LPS (LPS)], mixed linear models were used. The adjustment of the covariance matrix and data distribution to choose the best model was performed by the smallest AIC, using the REML estimator. For all analyses, $\alpha = 0.05$ was adopted. The unfolding of interactions was performed using the adjusted Bonferroni test. Original means and standard deviations were shown in the supplementary tables to facilitate the interpretation of the results. The variable members did not fit in the model; thus, non-parametric tests such as Mann-Whitney were applied to compare groups with or without LPS, within each brain region in each type of Hedgehog Pathway Members. The Friedman test was used to compare the brain regions, and the Kruskal-Wallis test was applied to compare the Shh members, within the same treatment group and the same region. All multiple comparisons were adjusted using the Bonferroni method. The SPSS statistical program was used. 25 (IBM) with $\alpha = 0.05$. The graphs were generated using the GraphPad Prism 7® program.

Ethics approval

This study was ethically reviewed and conducted in accordance with ethical guidelines of the Ethics Committee for Animal Research (PP00760/CEUA) of the Universidade Federal de Santa Catarina, Florianópolis, Brazil.

Consent for publication

All the authors agree to the publication of this work.

Availability of data and material

The datasets generated during and/or analyzed during the current study are available from the corresponding author on reasonable request.

Funding

This work was supported by São Paulo Research Foundation (FAPESP). MRC and AYIS acknowledges funding support from the FAPESP (Scientific Initiation Scholarship – grants numbers: FAPESP 2019/25772-2 and FAPESP 2019/21392-0).

CRediT authorship contribution statement

Mariana Ribeiro Costa: Data curation. **Amanda Yasmin Ilario dos Santos:** Data curation. **Taís Browne de Miranda:** Data curation. **Rogério Aires:** . **Alex de Camargo Coque:** . **Elizabeth Cristina Perez Hurtado:** . **Maria Martha Bernardi:** Writing – review & editing. **Vanessa Gallego Arias Pecorari:** Formal analysis, Investigation, Data curation, Writing – original draft. **Denise Carleto Andia:** Formal analysis, Investigation, Data curation, Writing – original draft. **Alexander Birbrair:** Conceptualization, Methodology, Formal analysis, Investigation, Writing – review & editing. **Gilles J. Guillemin:** Conceptualization, Methodology, Formal analysis, Investigation, Writing – review & editing. **Alexandra Latini:** Writing – review & editing, Conceptualization, Methodology, Formal analysis, Investigation. **Rodrigo A. da Silva:** Writing – review & editing, Conceptualization, Methodology, Formal analysis, Writing – review & editing.

Declaration of Competing Interest

The authors declare that they have no known competing financial interests or personal relationships that could have appeared to influence the work reported in this paper

Data availability

Data will be made available on request.

Acknowledgments

The authors are grateful to São Paulo Research Foundation (FAPESPF) and Research, Technology and Innovation Support Foundation of the University of Taubaté (Fapeti). The views expressed in this publication are those of the author(s) and not necessarily those of the FAPESP. We would like to thank Professor Gilles J. Guillemin of Macquarie University in Sydney/Australia for his comments on an earlier version of this manuscript.

Appendix A. Supplementary data

Supplementary data to this article can be found online at https://doi.org/10.1016/j.brainres.2022.148180.

References

Abg Abd Wahab, D.Y., Gau, C.H., Zakaria, R., Muthu Karuppan, M.K., A-rahbi, B.S., Abdullah, Z., Alrafiah, A., Abdullah, J.M., Muthuraju, S., 2019. Review on cross talk between neurotransmitters and neuroinflammation in striatum and cerebellum in the mediation of motor behaviour. Biomed. Res. Int. 2019, 1–10.

Alvarez-Buylla, A., Ihrie, R.A., 2014. Sonic hedgehog signaling in the postnatal brain. Semin. Cell Dev. Biol. 33, 105–111. https://doi.org/10.1016/j.semcdb.2014.05.008.
Amankulor, N.M., Hambardzumyan, D., Pyonteck, S.M., Becher, O.J., Joyce, J.A., Holland, E.C., 2009. Sonic hedgehog pathway activation is induced by acute brain injury and regulated by injury-related inflammation. J. Neurosci. 29, 10299–10308. https://doi.org/10.1523/JNEUROSCI.2500-09.2009.
Antonelli, Francesca, Arianna Casciati, Simonetta Pazzaglia, 2019. Sonic hedgehog signaling controls dentate gyrus patterning and adult neurogenesis in the hippocampus. Neural Regen. Res. 14, 59–61. https://doi.org/10.4103/1673-5374.243703.
Antunes, C., Da Silva, J.D., Guerra-Gomes, S., Alves, N.D., Ferreira, F., Loureiro-Campos, E., Branco, M.R., Sousa, N., Reik, W., Pinto, L., Marques, C.J., 2021. Tet3 ablation in adult brain neurons increases anxiety-like behavior and regulates cognitive function in mice. Mol. Psychiatry 26 (5), 1445–1457.
Bambakidis, N.C., Petrullis, M., Kui, X., Rothstein, B., Karampelas, I., Kuang, Y., Selman, W.R., LaManna, J.C., Miller, R.H., 2012. Improvement of neurological recovery and stimulation of neural progenitor cell proliferation by intrathecal administration of Sonic hedgehog. J. Neurosurg. 116, 1114–1120. https://doi.org/10.3171/2012.1.JNS111285.
Bhutani, N., Burns, D.M., Blau, H.M., 2011. DNA demethylation dynamics. Cell 146, 866–872. https://doi.org/10.1016/j.cell.2011.08.042.
Biesmans, S., Meert, T.F., Bouwknecht, J.A., Acton, P.D., Davoodi, N., De Haes, P., Kuijlaars, J., Langlois, X., Matthews, L.J.R., Ver Donck, L., Hellings, N., Nuydens, R., 2013. Systemic immune activation leads to neuroinflammation and sickness behavior in mice. Mediators Inflamm. 2013.
Boersma, G.J., Lee, R.S., Cordner, Z.A., Ewald, E.R., Purcell, R.H., Moghadam, A.A., Tamashiro, K.L., 2014. Prenatal stress decreases Bdnf expression and increases methylation of Bdnf exon IV in rats. Epigenetics 9, 437–447. https://doi.org/10.4161/epi.27558.
Bohannon, D.G., Ko, A., Filipowicz, A.R., Kuroda, M.J., Kim, W.-K., 2019. Dysregulation of sonic hedgehog pathway and pericytes in the brain after lentiviral infection. J. Neuroinflam. 16, 86. https://doi.org/10.1186/s12974-019-1463-y.
Carella, A., Tejedor, J.R., García, M.G., Urdinguio, R.G., Bayón, G.F., Sierra, M., López, V., García-Toraño, E., Santamarina-Ojeda, P., Pérez, R.F., Bigot, T., Mangas, C., Corte-Torres, M.D., Sáenz-de-Santa-María, I., Mollejo, M., Meléndez, B., Astudillo, A., Chiara, M.D., Fernández, A.F., Fraga, M.F., 2020. Epigenetic downregulation of TET3 reduces genome-wide 5hmC levels and promotes glioblastoma tumorigenesis. Int. J. cancer 146, 373–387. https://doi.org/10.1002/ijc.32520.
Carrillo-Jimenez, A., Deniz, Ö., Niklison-Chirou, M.V., Ruiz, R., Bezerra-Salomão, K., Stratoulias, V., Amouroux, R., Yip, P.K., Vilalta, A., Cheray, M., Scott-Egerton, A.M., Rivas, E., Tayara, K., García-Domínguez, I., Garcia-Revilla, J., Fernandez-Martin, J. C., Espinosa-Oliva, A.M., Shen, X., St George-Hyslop, P., Brown, G.C., Hajkova, P., Joseph, B., Venero, J.L., Branco, M.R., Burguillos, M.A., 2019. TET2 regulates the neuroinflammatory response in microglia. Cell Rep. 29, 697–713.e8. https://doi.org/10.1016/j.celrep.2019.09.013.
Charytoniuk, D., Porcel, B., Rodríguez Gomez, J., Faure, H., Ruat, M., Traiffort, E., 2002. Sonic Hedgehog signalling in the developing and adult brain. J. Physiol. Paris 96 (1-2), 9–16.
Chen, S.-D., Yang, J.-L., Hwang, W.-C., Yang, D.-I., 2018. Emerging roles of sonic hedgehog in adult neurological diseases: neurogenesis and beyond. Int. J. Mol. Sci. 19 (8), 2423.
Cui, D.i., Xu, X., 2018. Dna methyltransferases, dna methylation, and age-associated cognitive function. Int. J. Mol. Sci. 19 (5), 1315.
Dai, R.-L., Zhu, S.-Y., Xia, Y.-P., Mao, L., Mei, Y.-W., Yao, Y.-F., Xue, Y.-M., Hu, B., 2011. Sonic hedgehog protects cortical neurons against oxidative stress. Neurochem. Res. 36, 67–75. https://doi.org/10.1007/s11064-010-0264-6.
Dantzer, R., O'Connor, J.C., Freund, G.G., Johnson, R.W., Kelley, K.W., 2008. From inflammation to sickness and depression: when the immune system subjugates the brain. Nat. Rev. Neurosci. 9, 46–56. https://doi.org/10.1038/nrn2297.
Dashti, M., Peppelenbosch, M.P., Rezaee, F., 2012. Hedgehog signalling as an antagonist of ageing and its associated diseases. Bioessays 34, 849–856. https://doi.org/10.1002/bies.201200049.
de Paula Martins, R., Glaser, V., Aguiar, A.S.J., de Paula Ferreira, P.M., Ghisoni, K., da Luz Scheffer, D., Lanfumey, L., Raisman-Vozari, R., Corti, O., De Paul, A.L., da Silva, R.A., Latini, A., 2018. De novo tetrahydrobiopterin biosynthesis is impaired in the inflammed striatum of parkin((-/-)) mice. Cell Biol. Int. 42, 725–733. https://doi.org/10.1002/cbin.10969.
Doheny, D., Manore, S.G., Wong, G.L., Lo, H.-W., 2020. Hedgehog signaling and truncated GLI1 in cancer. Cells 9 (9), 2114.
Dunn, A.J., 2006. Effects of cytokines and infections on brain neurochemistry. Clin. Neurosci. Res. 6, 52–68. https://doi.org/10.1016/j.cnr.2006.04.002.
Edwards, J.R., Yarychkivska, O., Boulard, M., Bestor, T.H., 2017. DNA methylation and DNA methyltransferases. Epigenetics Chromatin 10, 23. https://doi.org/10.1186/s13072-017-0130-8.
Ghisoni, K., Martins, R.d.P., Barbeito, L., Latini, A., 2015. Neopterin as a potential cytoprotective brain molecule. J. Psychiatr. Res. 71, 134–139.
Gontier, G., Iyer, M., Shea, J.M., Bieri, G., Wheatley, E.G., Ramalho-Santos, M., Villeda, S.A., 2018. Tet2 rescues age-related regenerative decline and enhances cognitive function in the adult mouse brain. Cell Rep. 22, 1974–1981. https://doi.org/10.1016/j.celrep.2018.02.001.
Hammerschmidt, M., Brook, A., McMahon, A.P., 1997. The world according to hedgehog. Trends Genet. 13, 14–21.
Han, Y.-G., Spassky, N., Romaguera-Ros, M., Garcia-Verdugo, J.-M., Aguilar, A., Schneider-Maunoury, S., Alvarez-Buylla, A., 2008. Hedgehog signaling and primary cilia are required for the formation of adult neural stem cells. Nat. Neurosci. 11, 277–284. https://doi.org/10.1038/nn2059.
Henry, C.J., Huang, Y., Wynne, A.M., Godbout, J.P., 2009. Peripheral lipopolysaccharide (LPS) challenge promotes microglial hyperactivity in aged mice that is associated with exaggerated induction of both pro-inflammatory IL-1beta and anti-inflammatory IL-10 cytokines. Brain. Behav. Immun. 23, 309–317. https://doi.org/10.1016/j.bbi.2008.09.002.
Hoogland, I.C.M., Houbolt, C., van Westerloo, D.J., van Gool, W.A., van de Beek, D., 2015. Systemic inflammation and microglial activation: systematic review of animal experiments. J. Neuroinflammation 12, 114. https://doi.org/10.1186/s12974-015-0332-6.
Ingham, P.W., McMahon, A.P., 2001. Hedgehog signaling in animal development: paradigms and principles. Genes Dev. 15, 3059–3087. https://doi.org/10.1101/gad.938601.
Jeng, K.-S., Chang, C.-F., Lin, S.-S., 2020. Sonic Hedgehog signaling in organogenesis, tumors, and tumor microenvironments. Int. J. Mol. Sci. 21 (3), 758.
Jurkowska, R.Z., Jurkowski, T.P., Jeltsch, A., 2011. Structure and function of mammalian DNA methyltransferases. Chembiochem 12, 206–222. https://doi.org/10.1002/cbic.201000195.
Kirsten, T.B., Silva, E.P., Biondi, T.F., Rodrigues, P.S., Cardoso, C.V., Massironi, S.M.G., Mori, C.M.C., Bondan, E.F., Bernardi, M.M., 2022. Bate palmas mutant mice as a model of Kabuki syndrome: Higher susceptibility to infections and vocalization impairments? J. Neurosci. Res. 100, 1438–1451. https://doi.org/10.1002/jnr.25050.
Kohli, R.M., Zhang, Y., 2013. TET enzymes, TDG and the dynamics of DNA demethylation. Nature 502, 472–479. https://doi.org/10.1038/nature12750.
Lee, D.-Y., Lee, C.-I., Lin, T.-E., Lim, S.H., Zhou, J., Tseng, Y.-C., Chien, S., Chiu, J.-J., 2012. Role of histone deacetylases in transcription factor regulation and cell cycle modulation in endothelial cells in response to disturbed flow. Proc. Natl. Acad. Sci. U. S. A. 109, 1967–1972. https://doi.org/10.1073/pnas.1121214109.
Marigo, V., Johnson, R.L., Vortkamp, A., Tabin, C.J., 1996. Sonic hedgehog differentially regulates expression of GLI and GLI3 during limb development. Dev. Biol. 180, 273–283. https://doi.org/10.1006/dbio.1996.0300.
Matt, S.M., Zimmerman, J.D., Lawson, M.A., Bustamante, A.C., Uddin, M., Johnson, R. W., 2018. Inhibition of DNA methylation with zebularine alters lipopolysaccharide-induced sickness behavior and neuroinflammation in mice. Front. Neurosci. 12, 636. https://doi.org/10.3389/fnins.2018.00636.
Millett, C.E., Phillips, B.E., Saunders, E.F.H., 2019. The sex-specific effects of LPS on depressive-like behavior and oxidative stress in the hippocampus of the mouse. Neuroscience 399, 77–88. https://doi.org/10.1016/j.neuroscience.2018.12.008.
Montalbán-Loro, R., Lozano-Ureña, A., Ito, M., Krueger, C., Reik, W., Ferguson-Smith, A. C., Ferrón, S.R., 2019. TET3 prevents terminal differentiation of adult NSCs by a non-catalytic action at Snrpn. Nat. Commun. 10, 1726. https://doi.org/10.1038/s41467-019-09665-1.
Murdoch, J.N., Copp, A.J., 2010. The relationship between sonic Hedgehog signaling, cilia, and neural tube defects. Birth Defects Res. A. Clin. Mol. Teratol. 88, 633–652. https://doi.org/10.1002/bdra.20686.
Nascimento, A., Bernardi, M., Pecorari, V., Massoco, C., Felicio, L., 2013. Temporal analysis of lipopolysaccharide-induced sickness behavior in virgin and lactating female rats. Neuroimmunomodulation 20, 305–312. https://doi.org/10.1159/000350705.
Noh, H., Jeon, J., Seo, H., 2014. Systemic injection of LPS induces region-specific neuroinflammation and mitochondrial dysfunction in normal mouse brain. Neurochem. Int. 69, 35–40. https://doi.org/10.1016/j.neuint.2014.02.008.
Northcott, P.A., Robinson, G.W., Kratz, C.P., Mabbott, D.J., Pomeroy, S.L., Clifford, S.C., Rutkowski, S., Ellison, D.W., Malkin, D., Taylor, M.D., Gajjar, A., Pfister, S.M., 2019. Medulloblastoma. Nat. Rev. Dis. Prim. 5, 11. https://doi.org/10.1038/s41572-019-0063-6.
Pagiatakis, C., Musolino, E., Gornati, R., Bernardini, G., Papait, R., 2021. Epigenetics of aging and disease: a brief overview. Aging Clin. Exp. Res. 33, 737–745. https://doi.org/10.1007/s40520-019-01430-0.
Pérez-Domínguez, M., Tovar-Y-Romo, L.B., Zepeda, A., 2018. Neuroinflammation and physical exercise as modulators of adult hippocampal neural precursor cell behavior. Rev. Neurosci. 29, 1–20. https://doi.org/10.1515/revneuro-2017-0024.
Petrova, R., Joyner, A.L., 2014. Roles for Hedgehog signaling in adult organ homeostasis and repair. Development 141, 3445–3457. https://doi.org/10.1242/dev.083691.
Pfeifer, G.P., Kadam, S., Jin, S.-G., 2013. 5-hydroxymethylcytosine and its potential roles in development and cancer. Epigenetics Chromatin 6, 10. https://doi.org/10.1186/1756-8935-6-10.
Pitter, K.L., Tamagno, I., Feng, X., Ghosal, K., Amankulor, N., Holland, E.C., Hambardzumyan, D., 2014. The SHH/Gli pathway is reactivated in reactive glia and drives proliferation in response to neurodegeneration-induced lesions. Glia 62, 1595–1607. https://doi.org/10.1002/glia.22702.
Placzek, M., Briscoe, J., 2018. Sonic hedgehog in vertebrate neural tube development. Int. J. Dev. Biol. 62, 225–234. https://doi.org/10.1387/ijdb.170293jb.
Rivell, A., Petralia, R.S., Wang, Y.-X., Clawson, E., Moehl, K., Mattson, M.P., Yao, P.J., 2019. Sonic hedgehog expression in the postnatal brain. Biol. Open 8. https://doi.org/10.1242/bio.040592.
Santiago, M., Antunes, C., Guedes, M., Iacovino, M., Kyba, M., Reik, W., Sousa, N., Pinto, L., Branco, M.R., Marques, C.J., 2020. Tet3 regulates cellular identity and DNA methylation in neural progenitor cells. Cell. Mol. Life Sci. 77, 2871–2883. https://doi.org/10.1007/s00018-019-03335-7.
Sasaki, H., Hui, C., Nakafuku, M., Kondoh, H., 1997. A binding site for Gli proteins is essential for HNF-3beta floor plate enhancer activity in transgenics and can respond to Shh in vitro. Development 124, 1313–1322.

Scheffer, D.d.L., Ghisoni, K., Aguiar, A.S., Latini, A., 2019. Moderate running exercise prevents excessive immune system activation. Physiol. Behav. 204, 248–255.
Shahi, M.H., Afzal, M., Sinha, S., Eberhart, C.G., Rey, J.A., Fan, X., Castresana, J.S., 2010. Regulation of sonic hedgehog-GLI1 downstream target genes PTCH1, Cyclin D2, Plakoglobin, PAX6 and NKX2.2 and their epigenetic status in medulloblastoma and astrocytoma. BMC Cancer 10, 614. https://doi.org/10.1186/1471-2407-10-614.
Shahi, M.H., Zazpe, I., Afzal, M., Sinha, S., Rebhun, R.B., Melendez, B., Rey, J.A., Castresana, J.S., 2015. Epigenetic regulation of human hedgehog interacting protein in glioma cell lines and primary tumor samples. Tumour Biol. 36, 2383–2391. https://doi.org/10.1007/s13277-014-2846-4.
Sims, J.R., Lee, S.-W., Topalkara, K., Qiu, J., Xu, J., Zhou, Z., Moskowitz, M.A., 2009. Sonic hedgehog regulates ischemia/hypoxia-induced neural progenitor proliferation. Stroke 40, 3618–3626. https://doi.org/10.1161/STROKEAHA.109.561951.
Singh, P., Konar, A., Kumar, A., Srivas, S., Thakur, M.K., 2015. Hippocampal chromatin-modifying enzymes are pivotal for scopolamine-induced synaptic plasticity gene expression changes and memory impairment. J. Neurochem. 134, 642–651. https://doi.org/10.1111/jnc.13171.
Sirko, S., Behrendt, G., Johansson, P.A., Tripathi, P., Costa, M., Bek, S., Heinrich, C., Tiedt, S., Colak, D., Dichgans, M., Fischer, I.R., Plesnila, N., Staufenbiel, M., Haass, C., Snapyan, M., Saghatelyan, A., Tsai, L.-H., Fischer, A., Grobe, K., Dimou, L., Gotz, M., 2013. Reactive glia in the injured brain acquire stem cell properties in response to sonic hedgehog. Cell Stem Cell 12, 426–439. https://doi.org/10.1016/j.stem.2013.01.019.
Sun, Z.-H., Liu, Y.-H., Liu, J., Xu, D.-D., Li, X.-F., Meng, X.-M., Ma, T.-T., Huang, C., Li, J., 2017. MeCP2 regulates PTCH1 expression through DNA methylation in rheumatoid arthritis. Inflammation 40, 1497–1508. https://doi.org/10.1007/s10753-017-0591-8.
Szwagierczak, A., Bultmann, S., Schmidt, C.S., Spada, F., Leonhardt, H., 2010. Sensitive enzymatic quantification of 5-hydroxymethylcytosine in genomic DNA. Nucleic Acids Res. 38 (19).
Toni, L.S., Garcia, A.M., Jeffrey, D.A., Jiang, X., Stauffer, B.L., Miyamoto, S.D., Sucharov, C.C., 2018. Optimization of phenol-chloroform RNA extraction. Optimization of phenol-chloroform RNA extraction. MethodsX 5, 599–608.
Traiffort, E., Charytoniuk, D., Watroba, L., Faure, H., Sales, N., Ruat, M., 1999. Discrete localizations of hedgehog signalling components in the developing and adult rat nervous system. Eur. J. Neurosci. 11, 3199–3214. https://doi.org/10.1046/j.1460-9568.1999.00777.x.
Tukachinsky, H., Lopez, L.V., Salic, A., 2010. A mechanism for vertebrate Hedgehog signaling: recruitment to cilia and dissociation of SuFu-Gli protein complexes. J. Cell Biol. 191, 415–428. https://doi.org/10.1083/jcb.201004108.
Varjosalo, M., Taipale, J., 2008. Hedgehog: functions and mechanisms. Genes Dev. 22, 2454–2472. https://doi.org/10.1101/gad.1693608.
Vichaya, E.G., Gross, P.S., Estrada, D.J., Cole, S.W., Grossberg, A.J., Evans, S.E., Tuvim, M.J., Dickey, B.F., Dantzer, R., 2019. Lipocalin-2 is dispensable in inflammation-induced sickness and depression-like behavior. Psychopharmacology (Berl). 236, 2975–2982. https://doi.org/10.1007/s00213-019-05190-7.
Williams, K., Christensen, J., Pedersen, M.T., Johansen, J.V., Cloos, P.A.C., Rappsilber, J., Helin, K., 2011. TET1 and hydroxymethylcytosine in transcription and DNA methylation fidelity. Nature 473, 343–348. https://doi.org/10.1038/nature10066.
Wils, L.J., Bijlsma, M.F., 2018. Epigenetic regulation of the Hedgehog and Wnt pathways in cancer. Crit. Rev. Oncol. Hematol. 121, 23–44. https://doi.org/10.1016/j.critrevonc.2017.11.013.
Wilson, V.L., Smith, R.A., Ma, S., Cutler, R.G., 1987. Genomic 5-methyldeoxycytidine decreases with age. J. Biol. Chem. 262 (21), 9948–9951.
Yang, C., Qi, Y., Sun, Z., 2021. The role of sonic hedgehog pathway in the development of the central nervous system and aging-related neurodegenerative diseases. Front. Mol. Biosci. 8, 711710 https://doi.org/10.3389/fmolb.2021.711710.
Yao, P.J., Petralia, R.S., Mattson, M.P., 2016. Sonic hedgehog signaling and hippocampal neuroplasticity. Trends Neurosci. 39, 840–850. https://doi.org/10.1016/j.tins.2016.10.001.
Yu, H., Su, Y., Shin, J., Zhong, C., Guo, J.U., Weng, Y.-L., Gao, F., Geschwind, D.H., Coppola, G., Ming, G., Song, H., 2015. Tet3 regulates synaptic transmission and homeostatic plasticity via DNA oxidation and repair. Nat. Neurosci. 18, 836–843. https://doi.org/10.1038/nn.4008.
Zhao, J., Bi, W., Xiao, S., Lan, X., Cheng, X., Zhang, J., Lu, D., Wei, W., Wang, Y., Li, H., Fu, Y., Zhu, L., 2019. Neuroinflammation induced by lipopolysaccharide causes cognitive impairment in mice. Sci. Rep. 9, 5790. https://doi.org/10.1038/s41598-019-42286-8.